

Scaling properties of driven interfaces in disordered media

Luís A. Nunes Amaral, Albert-László Barabási[†], Hernán A. Makse, and H. Eugene Stanley
Center for Polymer Studies and Dept. of Physics, Boston University, Boston, Massachusetts 02215
(August 7, 2018)

We perform a systematic study of several models that have been proposed for the purpose of understanding the motion of driven interfaces in disordered media. We identify two distinct universality classes: (i) One of these, referred to as directed percolation depinning (DPD), can be described by a Langevin equation similar to the Kardar-Parisi-Zhang equation, but with quenched disorder. (ii) The other, referred to as quenched Edwards-Wilkinson (QEW), can be described by a Langevin equation similar to the Edwards-Wilkinson equation but with quenched disorder. We find that for the DPD universality class the coefficient λ of the nonlinear term diverges at the depinning transition, while for the QEW universality class either $\lambda = 0$ or $\lambda \rightarrow 0$ as the depinning transition is approached. The identification of the two universality classes allows us to better understand many of the results previously obtained experimentally and numerically. However, we find that some results cannot be understood in terms of the exponents obtained for the two universality classes *at* the depinning transition. In order to understand these remaining disagreements, we investigate the scaling properties of models in each of the two universality classes *above* the depinning transition. For the DPD universality class, we find for the roughness exponent $\alpha_P = 0.63 \pm 0.03$ for the pinned phase, and $\alpha_M = 0.75 \pm 0.05$ for the moving phase. For the growth exponent, we find $\beta_P = 0.67 \pm 0.05$ for the pinned phase, and $\beta_M = 0.74 \pm 0.06$ for the moving phase. Furthermore, we find an anomalous scaling of the prefactor of the width on the driving force. A new exponent $\varphi_M = -0.12 \pm 0.06$, characterizing the scaling of this prefactor, is shown to relate the values of the roughness exponents on both sides of the depinning transition. For the QEW universality class, we find that $\alpha_P \approx \alpha_M = 0.92 \pm 0.04$ and $\beta_P \approx \beta_M = 0.86 \pm 0.03$ are roughly the same for both the pinned and moving phases. Moreover, we again find a dependence of the prefactor of the width on the driving force. For this universality class, the exponent $\varphi_M = 0.44 \pm 0.05$ is found to relate the different values of the local α_P and global roughness exponent $\alpha_G \approx 1.23 \pm 0.04$ at the depinning transition. These results provide us with a more consistent understanding of the scaling properties of the two universality classes, both at and above the depinning transition. We compare our results with all the relevant experiments.

PACS numbers: 47.55.Mh 68.35.Fx

I. INTRODUCTION

Recently the growth of rough interfaces has witnessed an explosion of theoretical, numerical, and experimental studies, fueled by the broad interdisciplinary aspects of the subject [1–6]. Applications can be so diverse as imbibition in porous media, fluid–fluid displacement, fire front motion, and the motion of flux lines in superconductors [7–17].

In general, a d -dimensional self-affine interface, described by a single-valued function $h(\mathbf{x}, t)$, evolves in a $(d + 1)$ -dimensional medium. Usually, some form of disorder η affects the motion of the interface leading to its roughening. Two main classes of disorder have been discussed in the literature. The first, called thermal or “annealed,” depends only on time. The second, referred to as “quenched,” is frozen in the medium. Early studies focused on *time-dependent* disorder as being responsible for the roughening [18–26]. Here, we consider in detail the effect of *quenched* disorder on the growth.

The presence of quenched disorder introduces an interesting analogy between the motion of driven interfaces in

disordered media and the theory of critical phenomena. The continual motion of the interface requires the application of a driving force F . There exists a critical force F_c , such that for $F < F_c$, the interface will become pinned by the disorder after some finite time. For $F > F_c$, the interface moves indefinitely with an average velocity $v(F)$. This suggests that the motion of driven rough interfaces in disordered media can be studied as a phase transition — which we shall call the *depinning transition*. The velocity of the interface v plays the role of the *order parameter*, since as $F \rightarrow F_c^+$, v vanishes as

$$v \sim f^\theta. \quad (1.1)$$

We call θ the *velocity* exponent, and $f \equiv (F - F_c)/F_c$ the *reduced force* (Fig. 1).

For $F \rightarrow F_c^+$, large but finite regions of the interface are pinned by the disorder. At the transition, the characteristic length ξ of these pinned regions diverges as

$$\xi \sim f^{-\nu}, \quad (1.2)$$

where ν is the *correlation length* exponent.

The added phenomenological richness introduced by the quenched disorder leads to an increased difficulty. In

fact, the problem of identifying the universality classes for interface roughening in the presence of quenched disorder and determining the corresponding sets of critical exponents has so far remain unsolved. Experimental and numerical measurements of some of the critical exponents vary considerably, and the question of the existence of universality classes has been raised [7–17,27–47]. The problem is made more complex by the disagreement of most experimentally measured values with analytical calculations [48–50].

In this paper, we address the question of why the same exponents vary in value for different systems. We study several numerical models introduced to study interface roughening in the presence of quenched disorder, and identify two universality classes. We show that one of those universality classes can be identified with the case studied analytically. The exponents for the other universality class cannot be determined from renormalization groups calculations. However, mappings to directed percolation (DP) and isotropic percolation allow us to estimate most scaling exponents.

The identification of the universality classes and the calculation of the respective scaling exponents *at* the depinning transition enable us to understand the results for most of the models proposed and for some of the experiments. We shall see that several experimental results — particularly for the case of the moving interface in fluid-fluid displacement experiments — still do not fit the framework provided by the universality classes we discuss. For this reason, we study models in each of the universality classes *above* the depinning transition — i.e., in the *moving* phase. The results obtained allow us to re-interpret the experimental measurements. Furthermore, we find that for one of the universality classes, some of the critical exponents change values at the depinning transition.

The paper is organized as follows: In Sec. II we introduce the problem, by describing the set of relevant scaling properties and associated exponents, for driven interfaces moving in disordered media. In Sec. III we discuss the experimental and numerical results motivated our study. In Sec. IV we consider several numerical models, and identify two distinct universality classes. In Sec. V we try to link the results obtained for the two universality classes with the experimental results. To achieve this goal, we study models, representative of each of the universality classes, above the depinning transition. Finally, in Sec. VI, we summarize our results and discuss some of the new questions arising from this work.

II. SCALING PROPERTIES AND CRITICAL EXPONENTS

An interface moving in a disordered medium becomes rough due to the action of the disorder. This roughening process can be quantified by studying the *global* interface width

$$W(L, t) \equiv \left\langle \left[\overline{h^2(\mathbf{x}, t)} - \overline{h(\mathbf{x}, t)}^2 \right]^{1/2} \right\rangle, \quad (2.1)$$

where L is the system size, the overbar denotes a spatial average, and the angular brackets denote an average over realizations of the disorder.

The study of discrete models [18–21] and continuum growth equations [22,23] leads to the observation that during the initial period of the growth, i.e. for $t \ll t_\times(L)$, the global width W grows with time as

$$W(t) \sim t^\beta \quad (t \ll t_\times), \quad (2.2)$$

where β is the *growth* exponent. For times much larger than t_\times the width saturates to a constant value. It was observed that the saturation width of the interface W_{sat} scales with L as

$$W_{\text{sat}} \sim L^\alpha \quad (t \gg t_\times), \quad (2.3)$$

where α is the *roughness* exponent.

The dependence of t_\times on L allows the combination of (2.2) and (2.3) into a single scaling law [18]

$$W(L, t) \sim L^\alpha f(t/t_\times) \quad (2.4a)$$

where

$$t_\times \sim L^z. \quad (2.4b)$$

Here $z = \alpha/\beta$ is the *dynamical* exponent, and $f(u)$ is a universal scaling function that grows as u^β when $u \ll 1$, and approaches a constant when $u \gg 1$.

An alternative way of determining the scaling exponents is to study the *local* width w in a box of length $\ell < L$. The scaling law (2.4), and the fact that the interface is self-affine (and with $\alpha < 1$), allow us to conclude

$$w(\ell, t) \sim \ell^\alpha f(\ell/\ell_\times), \quad (2.5a)$$

where

$$\ell_\times \sim t^{1/z} \quad (t \ll t_\times), \quad (2.5b)$$

or

$$\ell_\times \sim L \quad (t \gg t_\times). \quad (2.5c)$$

Here $f(u)$ is a universal scaling function that decreases as $u^{-\alpha}$ when $u \gg 1$ and approaches a constant when $u \ll 1$.

Not all of the exponents introduced so far are independent; e.g., we can calculate the velocity exponent from the other scaling exponents, as we show by the following argument. Near the depinning transition, except for a few growing regions, most of the interface is pinned by some pinning path. The growth occurs by the propagation of these growing regions through the system. The characteristic time required for this propagation must

be of the order of t_{\times} , since this is the time for correlations to propagate across the entire system, as defined by (2.4b). During this process the interface advances from one blocking path to the next, the distance advanced is typically of the order of W_{sat} . Since, close to the transition, $\xi \sim L$, we can use (1.2), (2.3), and (2.4) to obtain

$$v \sim W_{\text{sat}} / t_{\times} \sim \xi^{\alpha} / \xi^z \sim \xi^{\alpha-z} \sim f^{-\nu(\alpha-z)}. \quad (2.6)$$

Upon comparison with (1.1), we conclude that

$$\theta = \nu(z - \alpha). \quad (2.7)$$

This exponent ‘‘scaling law’’ can also be derived in a different way [49,50], by considering the interplay between the range of action of the quenched disorder and the length scales for which the disorder can be considered to be time-dependent because of the motion of the interface. The quenched disorder is a function of \mathbf{x} and h , but we can consider the change of variables to a reference frame moving with the velocity of the interface

$$\eta(x, h) \rightarrow \eta(x, vt + h). \quad (2.8)$$

Now, we can consider the conditions for which $vt \gg h$. This will happen for the length scale characterizing the action of the quenched disorder, ξ . Thus we have

$$v \sim h/t \sim \xi^{\alpha}/\xi^z \sim \xi^{\alpha-z} \sim f^{\nu(z-\alpha)}, \quad (2.9)$$

leading to (2.7).

III. DRIVEN INTERFACES IN DISORDERED MEDIA

A. Experiments

The most commonly measured exponent in experiments and simulations is the roughness exponent α . In the last few years, several experiments in which quenched disorder plays a dominant role have been performed.

(i) Stokes *et al.* performed fluid-fluid displacement experiments, and observed that for some conditions a self-affine interface would form, while for other, the growth would generate a percolation-like cluster [7].

(ii) Rubio *et al.* measured α for fluid-fluid displacement experiments [8], consistently obtaining 0.73 regardless of the velocity of the interface v . Moreover, they observed that the total width of the interface decreased with v [8].

(iii) Horváth *et al.* performed similar fluid-fluid displacement experiment, obtaining $\alpha \approx 0.81$ [9].

(iv) Buldyrev *et al.* studied the imbibition of coffee in paper towels observing $\alpha \approx 0.63$ for the pinned interface [12,13,16,17]. Similar experiments were performed by Buldyrev *et al.* for 2 + 1 dimensions leading to $\alpha \approx 0.52$ [14].

(v) He *et al.* conducted fluid-fluid displacements experiments for different velocities of the interface [10]. They reported values of α varying from 0.6 for high velocities, to 0.9 for low velocities. Furthermore, they also observed that the total width of the interface decrease with velocity [10].

(vi) Zhang *et al.* performed flameless paper burning experiments [11]. They reported $\alpha \approx 0.71$ for the moving interface.

Thus the experiments reveal values of the roughness exponent as low as 0.6 and as high as 0.9, leading many to question whether one can divide all systems into a small number of universality classes (Fig. 2).

B. Discrete models

Several discrete models with quenched disorder have been proposed to explain the experimental results.

(i) Early on, Cieplak and Robbins noticed the importance of quenched disorder in many surface phenomena [27]. They studied two models, motivated by fluid-fluid displacement experiments. The first, called the *fluid invasion model*, is a quite realistic model and calculations reveal $\alpha \approx 0.8$ in 1 + 1 dimensions [27,28]. The second, called the *random field Ising model* (RFIM) [48], does not have a self-affine phase in 1 + 1 dimensions, so no roughness exponent can be calculated. On the other hand, for 2 + 1 dimensions, a self-affine regime exists, and a roughness exponent of 0.66 was calculated [27,28].

(ii) Kessler *et al.* integrated the Edwards-Wilkinson (EW) equation with quenched disorder, with the purpose of explaining the results for the fluid-fluid displacement experiments [29]. They reported values of α that vary with the driving force, i.e. with the velocity of the interface. For low velocities they found $\alpha \approx 1$, and for large velocities, $\alpha \approx 0.5$ [29]. Furthermore, they found a decrease of the total width with the velocity of the interface. Similar results were obtained earlier by Koplik and Levine [30].

(iii) Buldyrev *et al.* introduced a discrete model to explain their imbibition experiments [12,13,17]. They found that in 1 + 1 dimensions the scaling behavior of the pinned interface can be obtained exactly by mapping the interface onto DP. In higher dimensions they found that the interface can be mapped onto a *directed surface* (DS) [14]. In 1 + 1 dimensions, DP and DS are equivalent, so this model is referred to as *directed percolation depinning* (DPD) model [14,17].

(iv) A similar model was introduced independently by Tang and Leschhorn [33]. For the DPD class of models, it was observed that $\alpha \approx 0.63$ for the pinned interface [12,13,33].

(v) Parisi also introduced a model for interface roughening; however, no measurement was made of the roughness exponent [31]. Several authors studied Parisi’s model and found it to possess problems (see Appendix

B). For this reason, Amaral introduced an alternate version of the model, which led to exponents identical to the ones obtained for the DPD class of models [32].

(vi) Dong *et al.* also integrated numerically the QEW equation, and reported $\alpha \approx 0.97$ from the study of the height-height correlation function [35].

(vii) Leschhorn introduced a model, corresponding essentially to a discretization of the QEW equation, and found $\alpha \approx 1.25$ from measurements of the global width. The disagreement with Ref. [35] was later explained by Leschhorn and Tang, by showing that the height-height correlation function is limited to a scaling with a roughness exponent smaller or equal to 1 [36].

(viii) Roux and Hansen studied what amounts to a self-organized version of Leschhorn's model finding that $\alpha \approx 0.86$ for the local width and $\alpha \approx 1.22$ for the global width [39]. Using a similar model, Galluccio and Zhang found identical results [40].

(x) Csahók *et al.* studied the effect of multiplicative quenched disorder in the scaling properties of the interface [41]. They found $\beta \approx 0.65$ and $\alpha \approx 0.8$, in close agreement with the experimental results of Horváth *et al.* [9].

C. Continuum models

On the continuum front, some attempts were made to explain the previous results. The first theoretical studies to introduce quenched disorder were performed independently by Nattermann *et al.* [49] and Narayan and Fisher [50]. Analyzing the Kardar-Parisi-Zhang (KPZ) equation [23] with quenched disorder, they argued that the dependence of the noise on $h(\mathbf{x}, t)$ introduces an infinite hierarchy of nonlinearities. They also noticed that in the annealed disorder case the KPZ nonlinearity has a kinematic origin. Thus $\lambda \sim v$, and λ should vanish at the depinning transition. For these reasons, they argue that at the depinning transition, it is sufficient to consider the equation [48,51]

$$\frac{\partial h}{\partial t} = F + \eta(\mathbf{x}, h) + \nabla^2 h, \quad (3.1)$$

where $\eta(\mathbf{x}, h)$ represents the quenched disorder. This equation was studied by means of the functional renormalization group [48–50], yielding to first order

$$\alpha = \epsilon/3, \quad (3.2a)$$

$$\nu = 1/(2 - \alpha), \quad (3.2b)$$

and

$$z = 2 - 2\epsilon/9, \quad (3.2c)$$

where $\epsilon \equiv 4 - d$. Hence $\alpha = 1$ in $1 + 1$ dimensions, in disagreement with many of the experimental and numerical results. Reference [50] also argued that all but (3.2c) are exact for all orders in ϵ .

In view of the disagreement between the theoretical predictions of the EW equation with quenched disorder and the results presented in the previous subsections, Csahók *et al.* numerically integrated the KPZ equation with quenched disorder [41]

$$\frac{\partial h}{\partial t} = F + \eta(\mathbf{x}, h) + \nabla^2 h + \lambda(\nabla h)^2. \quad (3.3)$$

The numerical integration of (3.3) for the *moving* phase [41] yielded exponents in agreement with the calculations for the models in the DPD universality class.

IV. THE DEPINNING TRANSITION

A. Looking for nonlinearities

The fact that for (3.1) we can calculate the exponents, and they do not agree with the numerical results obtained for (3.3), suggests that the nonlinear term $\lambda(\nabla h)^2$ may play a crucial role in determining the scaling properties of the interface. Unfortunately no analytical results are available for Eq. (3.3). In this section, we investigate the presence of the nonlinear term in several of the models discussed in the previous section [42].

If we consider an equation of the KPZ-type, and consider its average over the spatial coordinates, we obtain

$$v = \overline{\partial h / \partial t} = \overline{F + \eta + \nabla^2 h + \lambda(\nabla h)^2}. \quad (4.1)$$

Now, if we impose an average *tilt* to the interface, $m \equiv \overline{\nabla y}$, and make the transformation

$$h(x, t) \rightarrow y(x, t) \equiv h(x, t) + mx, \quad (4.2)$$

we obtain

$$v(m) = \overline{\partial y / \partial t} = \overline{F + \eta + \nabla^2 h + \lambda(\nabla h)^2} + \lambda m^2. \quad (4.3)$$

So, it follows that the average velocity of the interface changes with the tilt as [52]

$$v(m) = v + \lambda m^2. \quad (4.4)$$

Thus by varying the tilt m , we can study the presence of nonlinear terms in the growth equation and calculate the effective coefficient λ of a given model [52].

For discrete models the tilt can be easily implemented introducing *helicoidal* boundary conditions. In $1 + 1$ dimensions, we simply impose the condition, $h(0, t) = h(L, t) - Lm$ and $h(L + 1, t) = h(1, t) + Lm$. In $d + 1$ dimensions, we use the same boundary conditions, so that the tilt occurs only in one direction.

B. The DPD universality class

1. The DPD-1 model

We begin by applying the method described above to the model introduced by Tang and Leschhorn [33]. In $1 + 1$ dimensions, the interface becomes pinned by a DP cluster [13,33], and the critical dynamics is controlled by a divergent correlation length parallel to the interface $\xi \sim f^{-\nu}$, with $\nu \approx 1.73$. This model, referred to as “DPD-1”, excludes overhangs, and gives rise to a self-affine interface at the depinning transition, with a roughness exponent $\alpha \approx 0.63$.

In the DPD-1 model, in $1 + 1$ dimensions, we start from a horizontal interface at the bottom edge of a lattice of size L . At every site of the lattice we define a random, uncorrelated quenched variable, the noise η , with magnitude in the range $[0, 1]$. During the time evolution of the interface, we choose one of the L columns at random [53]. If the difference in height to the lowest neighbor is larger than $+1$, this lowest neighboring column grows by one unit. Otherwise, the chosen column grows one unit provided the noise on the site above the interface is smaller than the driving force F . The unit time is defined to be L growth attempts.

We measure the velocity of the interface for different values of the reduced force f and different values of the tilt m . The results for $1 + 1$ dimensions are shown in Fig. 3(a). For a fixed force f , we find that the interface velocity depends on the tilt m , indicating the existence of nonlinear terms. Near the depinning transition ($f \rightarrow 0$), the velocity curves become “steeper” and, from (4.4), we infer that λ is coupled to the external force and that it increases as $f \rightarrow 0$.

To measure λ , we first attempt to fit a parabola to the tilt-dependent velocities in the vicinity of zero tilt. The calculations indicate that as we approach the depinning transition, λ diverges as [42]

$$\lambda \sim f^{-\phi}. \quad (4.5)$$

However, in the vicinity of F_c , the velocity curves lose their parabolic shape for large tilts (see Figs. 3(a) and 4), indicating a change to a different universality class [43].

We can understand the breakdown of (4.4) for large m using scaling arguments. Substituting Eqs. (1.1) and (4.5) into (4.4), we find [42]

$$v(m, f) \propto f^\theta + af^{-\phi}m^2. \quad (4.6)$$

Equation (4.6) indicates that the velocity curves corresponding to two different forces f_1 and f_2 , with $f_1 > f_2$, will intersect at a tilt m_\times (see Fig. 4). For tilts greater than m_\times , $v(m, f_1) < v(m, f_2)$, a clearly unphysical prediction since $f_1 > f_2$, and since the average velocity, for the same tilt m , should be larger for the larger force. Thus the velocity cannot follow a parabola for arbitrarily large m , and a crossover to a different behavior than

that of Eq. (4.6) must occur for values of the tilt larger than m_\times .

Letting $(f_1 - f_2) \rightarrow 0$, we find from (4.6) that the crossing point of the two corresponding parabolas scales as

$$m_\times^2 \sim f^{\theta+\phi}. \quad (4.7)$$

Equations (4.6) and (4.7) motivate the scaling form for the velocities [42]

$$v(m, f) \sim f^\theta g(m^2/f^{\theta+\phi}), \quad (4.8)$$

where $g(x) \sim \text{const}$ for $x \ll 1$, and $g(x) \sim x^{\theta/(\theta+\phi)}$ for $x \gg 1$ [54]. Figure 3 shows the data collapse we obtain using (4.8), with the exponents

$$\theta = 0.64 \pm 0.08, \quad \phi = 0.64 \pm 0.08, \quad (4.9)$$

for $1 + 1$ dimensions. Below, we will show that an entire class of models produces similar results, which will allow us to group them into a single universality class.

2. Other models

The scaling behavior (4.8) is not limited to the DPD-1 model in $1 + 1$ dimensions. For $2 + 1$ dimensions and for the models introduced in Refs. [12,31,32], we find a very similar behavior (Table I).

The “DPD-2” model was introduced by Buldyrev *et al.* [12–14] (see also Amaral *et al.* [17]). Let us define the model for $1 + 1$ dimensions. In a square lattice of edge L , assign an uncorrelated random number, the disorder η_i , with magnitude uniformly distributed in the interval $[0, 1]$, to each cell i . We compare the random pinning forces η_i in the lattice with the driving force F , where $0 \leq F \leq 1$. If the pinning force at a certain cell η_i is larger than the driving force, the cell is labeled “blocked”, otherwise it is labeled “unblocked”. Thus a cell is blocked with a probability $p = 1 - F$.

Since the model was developed to study imbibition, we will refer to the growing, invading, region as “wet”, and to the invaded region as “dry”. At time $t = 0$, we wet all cells in the bottom row of the lattice. Then, we select a column at random [53], and wet all dry *unblocked cells* in that column that are nearest-neighbors to a wet cell. To obtain a single-valued interface, we impose the auxiliary rule that all dry *blocked cells* below a wet cell become wet as well [55]. We refer to this rule as *erosion of overhangs*. The time unit is defined as L growth attempts.

Figure 5 shows the dependence of the velocity on the tilt for the “DPD-2” model and the respective data collapse according to (4.8), for $1 + 1$ dimensions. The values of the exponents in the data collapse are [56]

$$\theta = 0.59 \pm 0.12, \quad \phi = 0.55 \pm 0.12. \quad (4.10)$$

Finally, we simulate the model proposed by Amaral [32], which we will refer to as “DPD-3”. We simulate it in $1+1$ dimensions, and rescale the tilt dependent velocities according to (4.8) using the exponents (Fig. 6)

$$\theta = 0.70 \pm 0.12, \quad \phi = 0.65 \pm 0.12. \quad (4.11)$$

3. Discussion

Three questions are raised by these results:

(i) Is the new exponent ϕ an independent exponent or can it be expressed in terms of the other known exponents?

(ii) What are the scaling properties of the tilted interface?

(iii) What are the reasons for the divergence of λ at the depinning transition?

Questions (i) and (ii) have recently been answered by Tang, Kardar and Dhar (TKD) [43]. They noticed that for the DPD class of models there is a characteristic slope

$$m_c = \xi_{\perp}/\xi_{\parallel} \sim f^{\nu(1-\alpha)}, \quad (4.12)$$

where ξ_{\perp} and ξ_{\parallel} are, respectively, the perpendicular and parallel correlation lengths of a DP cluster (see Appendix A).

For values of the average tilt smaller than m_c , the interface still belongs to the DPD universality class. However, for larger values of the tilt a qualitative change should occur. But we showed above that such a change occurs for $m > m_{\times}$, so we conclude that $m_c = m_{\times}$, from which follows [43]

$$\theta + \phi = 2\nu(1 - \alpha). \quad (4.13)$$

Combining (4.13) with (1.1), we find the scaling law

$$\phi = \nu(2 - \alpha - z). \quad (4.14)$$

TKD also showed that for $m > m_{\times}$ a *new* universality class is obtained [43], and they were able to relate its scaling exponents to the exponents of the KPZ equation with annealed disorder [43]

$$\alpha_d = \alpha_{d-1}^{\text{KPZ}}/z_{d-1}^{\text{KPZ}}, \quad z_d = 1/z_{d-1}^{\text{KPZ}}. \quad (4.15)$$

To address question (iii), let us consider the effect of the nonlinear term. Its role is to make the interface grow wherever it has a nonzero slope, so it corresponds to what we can refer to as lateral growth. When an interface is moving, we can consider two types of growth, forward growth and lateral growth. The meaning of $\lambda \rightarrow \infty$ is then the irrelevance of forward growth compared with lateral growth when we approach the depinning transition. These ideas were studied quantitatively by Makse [57], who found that, near the depinning transition, the probability of occurrence of lateral growth vanishes much slower than the probability of occurrence of

forward growth. Furthermore, Makse argued that the application of constraints to the local slopes of the interfaces, as is the case for the DPD class of models, appears to be an *essential* ingredient for λ to diverge [57].

C. The QEW universality class

1. Discretizations of the QEW equation

We mentioned in Sec. III that several authors numerically integrated Eq. (3.1), and others developed models corresponding to the discretization of this equation. Thus, we expect results in agreement with the theoretical calculations. Furthermore, we do not expect, for these models, to detect any dependence of the velocity on the tilt of the interface. In fact, we have simulated the model introduced by Leschhorn [34], which we will refer to as “QEW-1”, and find that for any reduced force, $\lambda = 0$ (Fig. 7).

A Hamiltonian model, which we will refer to as “QEW-2”, was introduced by Makse [46]. In $1+1$ dimensions, the Hamiltonian is defined as

$$\mathcal{H} = \sum_{i=1}^L [(h_{i+1} - h_i)^2 - Fh_i + \zeta(i, h_i)]. \quad (4.16)$$

Here, the first term represents the elastic energy that tends to smooth the interface, and $\zeta(i, h_i)$ is an uncorrelated random number which mimics a random potential due to the disorder of the medium. In the simulation, a column i is chosen and its height is updated to $(h_i + 1)$ if the change in (4.16) is negative. Thus, only motions that decrease the total energy of the system are accepted. Backward motions are neglected since these are rare events. Equation (3.1) can be easily derived from this Hamiltonian simply by considering that

$$\frac{\partial h}{\partial t} = -\frac{\delta \mathcal{H}}{\delta h}, \quad \eta = -\frac{\delta \zeta}{\delta h}. \quad (4.17)$$

We study the dependence of the velocity with the tilt for this model and find that $\lambda = 0$ for any force, just as for the QEW-1 model.

2. The RFIM

An interesting result, presented in Sec. III, is the reasonable agreement between the exponents measured for the FIM and the RFIM [27,28] with the predictions of (3.1). Since these models are not simple discretizations of Eq. (3.1), it is interesting to investigate the presence of any nonlinear term.

For this reason, we study the RFIM in both $1+1$ and $2+1$ dimensions. This model allows for overhangs, and for certain values of its parameters can be mapped to the

isotropic percolation problem [28]. In the RFIM, spins on a square lattice interact through the Hamiltonian

$$\mathcal{H} \equiv - \sum_{\langle i,j \rangle} S_i S_j - \sum_i [F + \zeta(i, h)] S_i, \quad (4.18)$$

where $S_i = \pm 1$, F now denotes the external magnetic field, and ζ is the time-independent local random field (i.e., quenched noise) whose values are uniformly distributed in the interval $[-\Delta, \Delta]$. The strength of the quenched disorder is characterized by the parameter Δ . At time zero, all spins are “down”—except those in the first row, which are initially “up”. The interface consists of all down spins that are nearest-neighbors to an up spin. During the time evolution of the system, we flip any down spin that belongs to the interface and is “unstable,” i.e., whenever the flip will lower the total energy of the system. The control parameter of the depinning transition is the external magnetic field F ; the unit time corresponds to the parallel flipping of all unstable spins [58].

For $1 + 1$ dimensions, there are two morphologically-different regimes, depending on the strength Δ of the disorder (i.e., of the random fields). For $\Delta > 1.0$, the interface is self-similar (SS), while for $\Delta < 1.0$ it is faceted or flat (FA). For $2 + 1$ dimensions, there is again a FA regime ($\Delta < 2.4$), a SS regime ($\Delta > 3.4$), and also a self-affine (SA) regime in between ($2.4 < \Delta < 3.4$) [27]. The SA regime, which exists only for the case of $2 + 1$ dimensions, is the only regime of the RFIM for which either Eqs. (3.1) or (3.3) could apply. In the SS regime, overhangs in the interface are larger enough for the approximation of small slopes not to be valid. On the other hand, in the FA regime, lattice effects dominate the growth [60].

For the SA and SS regimes we find that (4.8) is still valid; however, we find a negative ϕ

$$\lambda \sim f^{|\phi|} \rightarrow 0. \quad (4.19)$$

This behavior can be understood, for the SS regime, by considering that near the depinning transition, the morphology of the interface corresponds to the hull of an isotropic percolation cluster, which has no well-defined orientation [27]. Thus a change in the boundary conditions will not affect the growth process, and we cannot expect any divergence of a possible nonlinear term when the magnetic field approaches its critical value. On the other hand, for large fields the effect of the quenched disorder diminishes, and we can observe an average interface orientation. For such values of field, we expect the presence of nonlinear terms, of *kinematic* origin, to be relevant. Although for the SA regime the behavior of λ is similar (Fig. 8), we do not have a simple argument that would explain the observed behavior.

These results lead us to conclude that in the SA regime the RFIM belongs to the universality class of Eq. (3.1). This conclusion is further supported by the agreement between the numerically determined exponents, $\alpha \approx 0.67$ and $\theta \approx 0.60$ for $2 + 1$ dimensions, and the theoretical predictions of (3.1).

D. Discussion

The results of Table I show, for $1 + 1$ dimensions, a separation into two groups in the values of the critical exponents for the six models studied [56]. This separation reflects the existence of two distinct universality classes, described by the two continuum growth equations, (3.1) and (3.3). For the QEW-1, QEW-2 models, and for the RFIM in the SA regime, we find that either $\lambda = 0$ or $\lambda \rightarrow 0$ at the depinning transition (Fig. 9). Thus, the scaling behavior of these models should be correctly described by (3.1). For the DPD-1, DPD-2, and DPD-3 models we observe a divergent λ , indicating that nonlinearities are relevant near the depinning transition. Thus to properly describe the scaling properties of these models it is necessary to study (3.3), since (3.1) does not include the nonlinear term $\lambda(\nabla h)^2$. Further evidence of the existence of the two universality classes is given by the values of the roughness exponents. The models for which λ diverges at the depinning transition, have $\alpha \approx 0.63$, in agreement with the mapping to DP [59]. On the other hand, models in the universality class of Eq. (3.1), gave roughness exponents typically larger, and in better agreement with the theoretical prediction, $\alpha \approx 1$.

It is worthwhile to discuss the implications of the previous results on other models and theoretical approaches studied in the literature. Recently, considerable attention has been focused on a self-organized version of the DPD model, the so-called self-organized depinning (SOD) model [12,17,61–65]. In this model, the constant driving force of the DPD model is replaced by an algorithm that selects the site on the interface for which the disorder is weakest — i.e, it selects the point in the interface offering the least resistance. Thus, the local update rule of the DPD model is replaced by a global search process, similar to the one used in invasion percolation. This update rule assures that the model will evolve to criticality and that it will remain in the critical state. This implies that the SOD model is always at the depinning transition. Thus the properties of the SOD model are described by the DPD model at criticality, which implies, since the SOD model is always at criticality, that the SOD model cannot be described by a continuum equation of the KPZ-type, since this would require an infinite coefficient of the nonlinear term. However, this argument *does not* rule out that the SOD model can be described by a continuum equation that upon a mapping to the quenched KPZ equation will generate an effective coefficient λ that would diverge [43].

V. THE MOVING PHASE

A. Why look at the moving phase?

In the previous section we identified the universality classes for interface roughening in the presence of quenched disorder. However, the experimental situation still leaves us with several unsolved puzzles, such as the change in the roughness exponent or the dependence of the global width on the driving force for the fluid-fluid displacement experiments.

In trying to shed some light over the remaining problems, we observe that most of the numerical and the analytical studies focus on the “pinned phase” ($F \leq F_c$) while nearly all experimental results are for the “moving phase” ($F > F_c$). A logical next step is therefore to study the moving phase for models representative of each of the two universality classes.

B. The DPD universality class

1. The steady state

Let us start by considering the DPD universality class. In Fig. 10(a), we show the local width for the pinned and the moving phases. We find $\alpha_P \approx 0.63$ for the pinned phase, and $\alpha_M \approx 0.75$ for the moving phase (Table II). So far, no explanation for this change in roughness exponent at the depinning transition is available.

The study of the scaling of the local width for the moving phase reveals a *novel* dependence of the prefactor of the width on the external force. We also find that the exponents characterizing this anomalous dependence change values for the two different regimes. In the first

$$w \sim \ell^{\alpha_M} f^{-\varphi_M} \quad (\ell \ll \xi), \quad (5.1)$$

where ξ is the correlation length, and φ_M is a new exponent that characterizes the dependence of the prefactor of the width on the driving force. In the second regime, the effect of the quenched disorder becomes irrelevant compared to the annealed disorder [53], and we obtain

$$w \sim \ell^{\alpha_A} f^{-\varphi_A} \quad (\ell \gg \xi), \quad (5.2)$$

where φ_A is a new exponent, and α_A is the roughness exponent corresponding to annealed disorder. Depending on the absence or presence of nonlinear terms, we recover the results of either the EW or the KPZ equations with annealed disorder. This crossover was observed both for experiments and simulations of discrete models [5].

Due to the dependence of the prefactor of the width on the driving force, and since $\xi \sim f^{-\nu}$, we propose the scaling *Ansatz*

$$w(\ell, f) \sim \ell^{\alpha_A} f^{-\varphi_A} g(\ell/\xi). \quad (5.3)$$

Upon comparison with (5.1) and (5.2), we find that the scaling function $g(u)$ satisfies $g(u \gg 1) \sim \text{const}$, and $g(u \ll 1) \sim u^{\alpha_M - \alpha_A}$. Using (5.3) we also obtain

$$\varphi_A = \varphi_M + \nu(\alpha_M - \alpha_A). \quad (5.4)$$

In Fig. 10(b) we show the data collapse of the widths for different forces and length scales. The deviations from scaling for large values of ℓ/ξ are due to finite-size effects (see Fig. 10(d) for discussion).

While previous studies considered α_M as an effective exponent, and concluded that no self-affine scaling exists in the moving phase for $\ell \ll \xi$ [33], we find a consistent value for α_M regardless of how closely we approach the depinning transition. The self-affinity of the interface is supported by the good data collapse obtained with (5.3), as shown in Fig. 10.

To derive a second relation for the new exponent φ_M , let us consider the approach to the depinning transition for a system of size L . For a finite system, the transition does not occur for $f = 0$, as it would for an infinite system, but rather for an effective critical force $F_c(L)$ such that $\xi \sim |F_c(L) - F_c|^{-\nu} \sim L$, implying $f \sim L^{-1/\nu}$. Using this result and (5.1), we obtain

$$w \sim \ell^{\alpha_M} L^{\varphi_M/\nu} \quad (\ell \ll L \sim \xi). \quad (5.5)$$

For the pinned phase we have

$$w \sim \ell^{\alpha_P} \quad (\ell \ll L \sim \xi). \quad (5.6)$$

At the depinning transition, (5.5) and (5.6) should scale in the same way. If we replace ℓ by L we obtain [67]

$$\varphi_M = \nu(\alpha_P - \alpha_M). \quad (5.7)$$

Replacing the known values of ν , α_P , α_M , and α_A into (5.4) and (5.7), we find

$$\varphi_M \approx -0.20, \quad \varphi_A \approx 0.23, \quad (5.8)$$

to be compared with the measured values $\varphi_M \approx -0.12$ and $\varphi_A \approx 0.34$ (Table II). Although the agreement with the measured values is not perfect, the error bars do not rule out the validity of (5.7).

2. The time evolution

For the DPD universality class, we find that β changes value at the depinning transition (see Table II). We find $\beta_P \approx 0.63$ for the pinned phase and $\beta_M \approx 0.75$ for the moving phase. We obtain for both sides of the transition $\alpha \approx \beta$, implying that z remains unchanged at the transition [68]. The exponent z characterizes the time scale t_x for the propagation of correlations in the interface (cf. Eq. (2.4)). This time scale is not expected to depend on the external force [44]. These results are in good agreement with a numerical integration of Eq. (3.3) [41].

For the time evolution of the width, we again find an anomalous dependence of the width on the reduced force for the two different scaling regimes. In regime I,

$$W \sim t^{\beta_M} f^{-\kappa_M} \quad (t \ll t_\times), \quad (5.9)$$

where $t_\times \sim \xi^z$ is the characteristic time for the propagation of correlations over a distance ξ , and κ_M is a new exponent that characterizes the dependence of the prefactor of the width on the driving force. In regime II, the effect of the pinned disorder becomes irrelevant compared to the annealed disorder [53], and we obtain

$$W \sim t^{\beta_A} f^{-\kappa_A} \quad (t \gg t_\times), \quad (5.10)$$

where κ_A is a new exponent, and β_A is the growth exponent corresponding to annealed disorder.

Since $t_\times \sim \xi^z \sim f^{-z\nu}$, we propose the scaling *Ansatz*

$$W(t, f) \sim t^{\beta_A} f^{-\kappa_A} g(t/t_\times). \quad (5.11)$$

Upon comparison with (5.9) and (5.10), we find that the scaling function $g(u)$ satisfies $g(u \gg 1) \sim \text{const}$, and $g(u \ll 1) \sim u^{\beta_M - \beta_A}$. From (5.11) we also obtain

$$\kappa_A = \kappa_M + z\nu(\beta_M - \beta_A). \quad (5.12)$$

In Fig. 11 we display the rescaling of our simulation results for the dependence of the global width on time and driving force according to (5.11).

To determine a second relation for the new exponent κ_M , let us again consider the approach to the depinning transition for a system of size L . As discussed above, the transition occurs for an effective critical force such that $\xi \sim L$, implying $f \sim L^{-1/\nu} \sim t_\times^{-1/z\nu}$. Using this result and (5.9), we obtain

$$W \sim t^{\beta_M} t_\times^{\kappa_M/z\nu} \quad (t \ll t_\times). \quad (5.13)$$

For the pinned phase, we have

$$W \sim t^{\beta_P} \quad (t \ll t_\times). \quad (5.14)$$

At the transition, (5.13) and (5.14) must scale in a similar way. So, if we replace t by t_\times , we obtain

$$\kappa_M = z\nu(\beta_P - \beta_M). \quad (5.15)$$

Replacing the known values of ν , z , β_P , β_M , and β_A into (5.12) and (5.15), we find

$$\kappa_M \approx -0.12, \quad \kappa_A \approx 0.64, \quad (5.16)$$

in good agreement with the simulation results, $\kappa_M \approx -0.11$ and $\kappa_A \approx 0.65$ (Table II).

C. The QEW universality class

1. The steady state

For the study of the QEW universality class, we focus on the QEW-2 model. We observe a dependence of the

local width on the system size L , that can be described by the scaling function [36,66]

$$w(\ell, L) \sim L^{\alpha_G} \Phi(\ell/L), \quad (5.17)$$

where $\Phi(u)$ is a scaling function that for $u \ll 1$ scales as u^{α_P} , and α_G is the global roughness exponent, which is defined by the scaling of the global width with the system size: $W \sim L^{\alpha_G}$. Equation (5.17) is valid only when $\alpha_G > 1$, and it implies that $w(\ell, L) \sim \ell^{\alpha_P} L^{\alpha_G - \alpha_P}$ for $\ell \ll L$. Hence, the local slopes are unbounded, i.e., they diverge with the system size. This anomalous characteristic of the QEW models is displayed in Fig. 12(a), where we plot interfaces generated for the QEW-2 model for different values of the system size. We calculate the global width as a function of L and find at the depinning transition that $\alpha_G \approx 1.23$.

We also determine the scaling of the local width w in a window of size ℓ , for different values of the reduced force. In Fig. 13(a), we show the local width for the pinned and the moving phases. Analysis of consecutive slopes yield roughness exponents $\alpha_P \approx 0.92$ for the pinned phase, and $\alpha_M \approx 0.92$ for the moving phase (Table II). These results are in agreement with values commonly found for the QEW class of models when the roughness exponent is calculated from the local width — i.e., $\alpha_P \approx \alpha_M \approx 1$. The slightly smaller value of our estimates is likely due to finite size effects.

As for the DPD universality class, the study of the local width in the moving phase reveals an anomalous dependence on the reduced force, which leads to Eqs. (5.3) and (5.4) being also valid for the QEW universality class. In Fig. 13(b), we show the data collapse of the local widths obtained using (5.3).

To determine a second relation for the new exponent φ_M , we again consider the approach to the depinning transition of a system of size L . As before, we obtain (5.5) for the moving phase. However, for the pinned phase, the scaling behavior (5.17), leads to

$$w \sim \ell^{\alpha_P} L^{\alpha_G - \alpha_P} \quad (\ell \ll L). \quad (5.18)$$

At the transition, (5.5) and (5.18) must be identical. Hence, we find

$$\alpha_P = \alpha_M, \quad (5.19a)$$

and

$$\varphi_M = \nu(\alpha_G - \alpha_P). \quad (5.19b)$$

Replacing the measured values of ν , α_G , α_P , and α_A into (5.4) and (5.19), we find

$$\varphi_M \approx 0.42, \quad \varphi_A \approx 1.04, \quad (5.20)$$

in good agreement with the values obtained in our simulations, $\varphi_M \approx 0.44$ and $\varphi_A \approx 0.99$ (Table II).

2. The time evolution

We study the scaling of W with t , and find $\beta_P \approx 0.85$ and $\beta_M \approx 0.86$. These results imply that z remains unchanged at the transition. In Fig. 14, we show the scaling of the global width as a function of time for different values of the reduced force, and its data collapse using (5.11).

For the QEW universality class, we find by replacing the measured values of ν , z , β_P , and β_A into (5.12) and (5.15) that

$$\kappa_M \approx 0.02, \quad \kappa_A \approx 1.19, \quad (5.21)$$

in good agreement with the values obtained in our simulations, $\kappa_M \approx 0$ and $\kappa_A \approx 1.15$ (Table II).

D. Discussion

The results obtained in the previous subsections allow us to discuss the experimental and numerical results reported in the literature. A problem with the interpretation of experimental and numerical results for the roughness exponent, has been the wide range of values for α : 0.5 – 1.25, measured in the moving phase. We note that, in this regime, the crossover to the annealed disorder regime leads to “effective” exponents that change with the velocity (or the driving force). For this reason, we suggest that the scaling function (5.3) might be useful in the determination of the exponents from the study of the local width w . As shown in Table II, the exponent φ_M has different signs for the two universality classes, leading to sharply distinct scaling behaviors for the prefactor of the width with the driving force. Since in many experiments it is possible to monitor the velocity of the interface, and therefore the driving force, the study of this prefactor may also lead to an easier identification of the universality class to which the experiments belong.

In light of this discussion, the interpretation of the results of Ref. [29] is clear. The numerical integration of the EW equation with quenched disorder performed in Ref. [29] must belong to the QEW universality class, and the reported exponents are “effective” exponents whose values were affected by the crossover to the annealed regime.

The determination of the universality class of the *fluid invasion model* (FIM) of Ref. [27,28] is not trivial. However, we note that ν is identical for the FIM and for the Hamiltonian model. On the other hand, the value of α measured in Ref. [27,28] is somewhat smaller than the value obtained for the QEW model using the local width.

Regarding the fluid-fluid displacement experiments of Refs. [7–10], we find that they share several scaling properties with the Hamiltonian model. We first notice that the range of roughness exponents measured in the experiments of Refs. [7–10] is consistent with the values that could be obtained with the Hamiltonian model. Moreover, Rubio *et al.* [7–10] found that the amplitude of

the width decreases with the increase of the velocity. This property is entirely consistent with our findings for the QEW universality class: if we replace $f \sim v^{1/\theta}$ in (5.1), then we obtain that the width decreases with v as $w \sim v^{-\varphi_M/\theta}$.

The imbibition experiments of Refs. [12,13,16] and the paper burning experiments of Ref. [11] are believed to belong to the DPD universality class. This conclusion is supported by the values of the exponents measured in both experiments.

The reason for the different universality classes for the two groups of experiments, fluid-fluid displacement on one hand and imbibition and paper burning on the other, is not totally clear. However, a possible explanation might be the importance of lateral growth in the second case compared with the first. When we analyze the imbibition and paper burning experiments, it becomes clear that the interface can be described by a single-valued interface, because only the highest position of the interface in each column is relevant for the dynamics. This effectively corresponds to eroding any overhangs and, as shown by Makse [57], leads to a diverging λ at the transition. On the other hand, in the fluid-fluid displacement experiments, we must at all times consider the full interface, because of the trapped fluid that might exist below the interface. Since it will require some effort to displace this fluid or to separate it from the rest of the displaced fluid, we cannot physically justify a rule such as the erosion of overhangs. This implies that λ vanishes at the depinning transition, and the experiments must belong to the QEW universality class.

VI. SUMMARY

To summarize, we perform a systematic study of several models proposed to understand the motion of driven interfaces in disordered media. We are able to identify *two* distinct universality classes. For one of these universality classes, QEW, we observe that it can be described by a Langevin equation similar to the EW equation but with quenched disorder. For the QEW universality class nearly all exponents for the pinned phase can be obtained by renormalization group calculations.

For the other universality class, DPD, we find that it can be described by a Langevin equation similar to the KPZ equation, but with quenched disorder. Furthermore, we find that the coefficient of the nonlinear term λ diverges at the depinning transition. Because of this divergence, no perturbative analytical calculations have been possible so far. However, a mapping of the static properties of the interface, at the depinning transition, to DP yields all static exponents of the problem. A mapping of the dynamics to isotropic percolation yields the dynamical exponent.

The identification of these two universality classes leads to some understanding of many of the results ob-

tained previously for models and experiments. However, many other results could not be understood in terms of the exponents obtained for the two universality classes *at* the depinning transition. For this reason, we also investigated the scaling properties of the models in the two universality classes *above* the depinning transition.

We find that for the DPD universality class, α and β change their values at the depinning transition. Furthermore, we find a dependence of the prefactor of the width on the driving force. The new exponent φ_M , characterizing the scaling of this prefactor, can be used to relate the values of the roughness exponents on both sides of the transition.

For the QEW universality class, we find that α and β remain unchanged at the depinning transition. As for the DPD universality class, we also find a dependence of the prefactor of the width on the driving force. The exponent φ_M is, in this case, found to relate the different values of the local, α_P , and global, α_G , roughness exponents at the depinning transition.

These results provide us with a more consistent understanding of the scaling properties of the two universality classes both at and above the depinning transition. This knowledge enables us to interpret most of the experimental results obtained previously. However, several questions, that demand an answer, are still unsolved. One of them is the reason for the change in values of the roughness exponent at the depinning transition for the DPD universality class. Another is the understanding of the different values of α_G and α_P for the QEW universality class.

ACKNOWLEDGMENTS

We thank S. V. Buldyrev, R. Cuerno, S. T. Harrington, S. Havlin, V. K. Horváth, P. Ch. Ivanov, K. B. Lauritsen, H. Leschhorn, I. Procaccia, P. Rey, R. Sadr, S. Tomassone, T. Vicsek, and P.-z. Wong for valuable contributions and discussions. L.A.N.A. acknowledges support from Junta Nacional de Investigação Científica e Tecnológica. The Center for Polymer Studies is supported by the National Science Foundation.

APPENDIX A: PREDICTING THE EXPONENTS OF THE DPD MODEL

1. Directed percolation

Near p_c , the size of DP clusters is characterized by a longitudinal (parallel) correlation length ξ_{\parallel} and a transverse (perpendicular) correlation length ξ_{\perp} that diverge as [70,71]

$$\xi_{\parallel} \sim |p_c - p|^{-\nu_{\parallel}}, \quad \xi_{\perp} \sim |p_c - p|^{-\nu_{\perp}}. \quad (\text{A1})$$

The parallel and perpendicular correlation length exponents for DP clusters have been calculated [72], with the results

$$\nu_{\parallel} = 1.733 \pm 0.001, \quad \nu_{\perp} = 1.097 \pm 0.001 \quad (d = 1). \quad (\text{A2})$$

2. Static properties

The mapping of the *pinned interface* to DP enables us to estimate the static exponents of this problem from the characteristic exponents of DP clusters. The characteristic length ξ of the pinned regions must be of the order of ξ_{\parallel} , so we can identify the exponent ν to be

$$\nu = \nu_{\parallel}. \quad (\text{A3})$$

The global width W_{sat} of the pinned interface should scale as ξ_{\perp} , since its advance is blocked by a DP path. On the other hand, ξ_{\parallel} must be larger than the system size L for the interface to become pinned, from which follows [12,13,33]

$$W_{\text{sat}} \sim \xi_{\perp} \sim \xi_{\parallel}^{\nu_{\perp}/\nu_{\parallel}} \sim L^{\nu_{\perp}/\nu_{\parallel}} \quad (\xi_{\parallel} \geq L). \quad (\text{A4})$$

Comparing with (2.3), we conclude that the roughness exponent is given in terms of the correlation exponents for DP,

$$\alpha = \nu_{\perp}/\nu_{\parallel}. \quad (\text{A5})$$

Substituting (A2) into (A5), we predict

$$\alpha = 0.633 \pm 0.001 \quad (d = 1). \quad (\text{A6})$$

3. The minimum path

For any fractal set with a fractal dimension smaller than the dimension of the embedding space, the distance between to points of the set ℓ is not given by the Euclidean distance r between those points but by the minimum path distance (or chemical distance) ℓ_{min} . Numerical studies show that ℓ_{min} scales as [70,71]

$$\ell_{\text{min}} \sim r^{d_{\text{min}}}, \quad (\text{A7})$$

where d_{min} is called the *minimum path* exponent.

4. Dynamical properties

Recently, Havlin *et al.* showed that the dynamics of the DPD model in $d + 1$ dimensions could be mapped to the minimum path of isotropic percolation in d dimensions [44]. They argued that close to the depinning transition only a few cells on the interface are active, i.e., unblocked. These active cells perform a global search of unblocked cells and propagate correlations in the interface. Since the cells through which the active cells can move are confined to unblocked or eroded blocked cells in a region of thickness $\xi_{\perp} \ll \xi_{\parallel}$, we can identify this region with an isotropic percolation cluster embedded in a space of dimension d .

Thus, the path through which active cells move is the minimum path. So, the time t for the correlations to propagate an Euclidean distance r , is proportional to ℓ_{\min} , which scales as $r^{d_{\min}}$ for isotropic percolation. From this follows that we can connect the dynamical exponent z to the static exponent d_{\min} of *isotropic* percolation [44]

$$z = d_{\min}. \quad (\text{A8})$$

APPENDIX B: THE DPD-3 MODEL

In this appendix, we discuss the model introduced by Parisi to study interface roughening in the presence of quenched disorder [31]. We show that the original growth rule leads to an unphysical behavior. We then proceed to describe the model proposed by Amaral that solves the problems with the original model [32].

Let us start by describing the model originally introduced by Parisi. In a square lattice of edge L , with periodic boundary conditions in that direction, we assign to each cell an uncorrelated random number, uniformly distributed in the interval $[-1, 1]$. We start, at $t = 0$, by invading the bottom row in the lattice, and then, we calculate the driving force for each column

$$F(i, t) = \rho \max[h(i \pm 1, t) + 1 - h(i, t)], \quad (\text{B1})$$

where ρ is the controlling parameter of the model. If this driving force F_i is larger than the noise in the cell above the interface, $\eta(i, h(i) + 1)$, then we update the height of column i to

$$h(i, t + 1) = \max[h(i \pm 1, t) + 1]. \quad (\text{B2})$$

The time evolution of this model leads to the development of huge jumps in the height of neighboring columns that propagate along the system. For small enough values of ρ , only one or two such growing regions will be propagating in the system. The reason for such “unnatural” behavior of the model is the growth rule (B2). The fact that the advancing column grows to a higher value than the highest neighbor is a kind of “bootstrap” that

is difficult to justify. In fact, it does not seem reasonable that any growth mechanism would pull a lower column to an height larger than that of its neighbors.

For this reason, Amaral proposed a new growth rule to replace (B2)

$$h(i, t + 1) = h(i, t) + 1. \quad (\text{B3})$$

In this way, the invading region only advances one cell at a time; thus, avoiding the formation of big jumps between neighboring columns [32].

The study of this model, which we will refer to as “DPD-3”, leads to the result that a critical value of the controlling parameter exists, $\rho_c = 0.196 \pm 0.002$. Below this threshold the interface stops moving after some finite time, and above it it moves indefinitely. To determine some of the scaling exponents, we applied the gradient method, introduced by Sapoval *et al.* [73], and already used in the study of the DPD-2 model [16,17] and in several other studies [74–76].

Figure 15 displays our results for the case of a linear gradient, $\nabla\rho(h) = g$. The scaling of the interface changes with the concentration rate and is characterized by an exponent γ according to

$$w(\ell, g) \sim \ell^{\alpha} f\left(\ell/g^{-\gamma/\alpha}\right) \quad (\text{B4})$$

where f is a universal scaling function that satisfies $f(x \ll 1) \sim \text{const}$, and $f(x \gg 1) \sim x^{-\alpha}$. Figure 15(a) shows the width w as a function of the size ℓ for different values of the concentration gradient g . Figure 15(b) shows the data collapse of these results according to (B4). The best collapse was obtained with the exponents

$$\alpha = 0.60 \pm 0.05, \quad \gamma = 0.49 \pm 0.05. \quad (\text{B5})$$

Since we know that [16]

$$\alpha = \nu_{\perp}/\nu_{\parallel}, \quad \gamma = \nu_{\perp}/(1 + \nu_{\perp}), \quad (\text{B6})$$

we obtain

$$\nu_{\perp} = 1.0 \pm 0.1, \quad \nu_{\parallel} = 1.6 \pm 0.1, \quad (\text{B7})$$

in agreement with the known results for DP [72].

† Present address: Department of Physics, University of Notre Dame, Notre Dame, IN 46556

[1] T. Vicsek, *Fractal Growth Phenomena*, 2nd ed., Part IV (World Scientific, Singapore, 1992); *Dynamics of Fractal Surfaces*, edited by F. Family and T. Vicsek (World Scientific, Singapore, 1991); J. Kertész and T. Vicsek, in *Fractals in Science*, edited by A. Bunde and S. Havlin (Springer-Verlag, Heidelberg, 1994).

- [2] J. Krug and H. Spohn, in *Solids Far From Equilibrium: Growth, Morphology and Defects*, edited by C. Godrèche (Cambridge University Press, Cambridge, 1991).
- [3] P. Meakin, Phys. Rep. **235**, 189 (1993).
- [4] T. Halpin-Healey and Y.-C. Zhang, Phys. Rep. **254**, 215 (1995).
- [5] A.-L. Barabási and H. E. Stanley, *Fractal Concepts in Surface Growth* (Cambridge University Press, Cambridge, 1995).
- [6] J.-F. Gouyet, M. Rosso and B. Sapoval, in *Fractals and Disordered Systems*, edited by A. Bunde and S. Havlin (Springer-Verlag, Heidelberg, 1991)
- [7] J. P. Stokes, A. P. Kushnick, and M. O. Robbins, Phys. Rev. Lett. **60**, 1386 (1988).
- [8] M. A. Rubio, C. A. Edwards, A. Dougherty, and J. P. Gollub, Phys. Rev. Lett. **63**, 1685 (1989); V. K. Horváth, F. Family, and T. Vicsek, *Ibid.* **65**, 1388 (1990), M. A. Rubio, C. A. Edwards, A. Dougherty, and J. P. Gollub, *Ibid.* **65**, 1389 (1990).
- [9] V. K. Horváth, F. Family, and T. Vicsek, J. Phys. A **24**, L25 (1991); Phys. Rev. Lett. **67**, 3207 (1991).
- [10] S. He, G. L. M. K. S. Kahanda and P.-z. Wong, Phys. Rev. Lett., **69**, 3731 (1992).
- [11] J. Zhang, Y.-C. Zhang, P. Alstrøm, M. T. Levinsen, Physica A **189**, 383 (1992).
- [12] S. Havlin, A.-L. Barabási, S. V. Buldyrev, C. K. Peng, M. Schwartz, H. E. Stanley, and T. Vicsek, in *Growth Patterns in Physical Sciences and Biology* [Proc. 1991 NATO Advanced Research Workshop, Granada], ed. J. M. Garcia-Ruiz, E. Louis, P. Meakin, and L. M. Sander (Plenum Press, New York, 1993).
- [13] S. V. Buldyrev, A.-L. Barabási, S. Havlin, F. Caserta, H. E. Stanley and T. Vicsek, Phys. Rev. A **45**, R8313 (1992).
- [14] S. V. Buldyrev, A.-L. Barabási, S. Havlin, J. Kertész, H. E. Stanley and H. S. Xenias, Physica A **191**, 220 (1992); A.-L. Barabási, S. V. Buldyrev, S. Havlin, G. Huber, H. E. Stanley, and T. Vicsek, in *Surface Disorder: Growth, Roughening and Phase Transitions*, ed. R. Jullien, J. Kertész, P. Meakin, and D. E. Wolf (Nova Science, New York, 1992).
- [15] S. V. Buldyrev, S. Havlin, and H. E. Stanley, Physica A **200**, 200 (1993); S. V. Buldyrev, S. Havlin, J. Kertész, A. Shehter, and H. E. Stanley, Fractals **1**, 827 (1993).
- [16] L. A. N. Amaral, A.-L. Barabási, S. V. Buldyrev, S. Havlin, and H. E. Stanley, Phys. Rev. Lett. **72**, 641 (1994); Fractals **1**, 818 (1993).
- [17] L. A. N. Amaral, A.-L. Barabási, S. V. Buldyrev, S. Havlin, S. T. Harrington, R. Sadr, and H. E. Stanley, Phys. Rev. E **51**, 4655 (1995).
- [18] F. Family and T. Vicsek, J. Phys A **18**, L75 (1985).
- [19] F. Family, J. Phys. A **19**, L441 (1986).
- [20] P. Meakin, P. Ramanlal, L. M. Sander, and R. C. Ball, Phys. Rev. A **34**, 5091 (1986).
- [21] J. M. Kim and J. M. Kosterlitz, Phys. Rev. Lett. **62**, 2289 (1989).
- [22] S. F. Edwards and D. R. Wilkinson, Proc. R. Soc. Lond. **A381**, 17 (1982).
- [23] M. Kardar, G. Parisi, and Y.-C. Zhang, Phys. Rev. Lett. **56**, 889 (1986).
- [24] E. Medina, T. Hwa, M. Kardar, and Y.-C. Zhang, Phys. Rev. A **39**, 3053 (1989); C. K. Peng, S. Havlin, M. Schwartz, and H. E. Stanley, Phys. Rev. A **44**, 2239 (1991); J. G. Amar, P.-M. Lam, and F. Family, Phys. Rev. A **43**, 4548 (1991).
- [25] Y.-C. Zhang, J. Physique **51**, 2129 (1990); S. V. Buldyrev, S. Havlin, J. Kertész, H. E. Stanley, and T. Vicsek, Phys. Rev. A **43**, 7113 (1991); S. Havlin, S. V. Buldyrev, H. E. Stanley, and G. H. Weiss, J. Phys. A **24**, L925 (1991).
- [26] A.-L. Barabási, Phys. Rev. A **46**, R2977 (1992).
- [27] M. Cieplak and M. O. Robbins, Phys. Rev. Lett. **60**, 2042 (1988); N. Martys, M. Cieplak, and M. O. Robbins, Phys. Rev. Lett. **66**, 1058 (1991).
- [28] C. S. Nolle, B. Koiller, N. Martys, and M. O. Robbins, Phys. Rev. Lett. **71**, 2074 (1993); B. Koiller, M. O. Robbins, H. Ji, and C. S. Nolle, in *New Trends in Magnetic Materials and their Applications*, edited by J. L. Moran-Lopez and J. M. Sanchez (Plenum, New York, 1993); M. O. Robbins, M. Cieplak, H. Ji, B. Koiller, and N. Martys, in *Growth Patterns in Physical Sciences and Biology*, edited by J. M. Garcia-Ruiz, E. Louis, P. Meakin, and L. M. Sander (Plenum, New York, 1993).
- [29] D. A. Kessler, H. Levine, Y. Tu, Phys. Rev. A **43**, 4551 (1991).
- [30] J. Koplik and H. Levine, Phys. Rev. B **32**, 280 (1985).
- [31] G. Parisi, Europhys. Lett. **17**, 673 (1992).
- [32] L. A. N. Amaral, Ph. D. Thesis, Boston University (1996).
- [33] L.-H. Tang and H. Leschhorn, Phys. Rev. A **45**, R8309 (1992).
- [34] H. Leschhorn, Physica A **195**, 324 (1993).
- [35] M. Dong, M. C. Marchetti, A. A. Middleton, and V. Vinokur, Phys. Rev. Lett. **70**, 662 (1993).
- [36] H. Leschhorn and L.-H. Tang, Phys. Rev. Lett. **70**, 2973 (1993).
- [37] M. Benoit and R. Jullien, Physica A **207**, 500 (1994).
- [38] D. Spasojevic and P. Alstrøm, Physica A **201**, 482 (1993).
- [39] S. Roux and A. Hansen, J. Phys. I France **4**, 515 (1994).
- [40] S. Galluccio and Y.-C. Zhang, Phys. Rev. E **51**, 1686 (1995).
- [41] Z. Csahók, K. Honda and T. Vicsek, J. Phys. A **26**, L171 (1993); Z. Csahók, K. Honda, E. Somfai, M. Vicsek and T. Vicsek, Physica A **200**, 136 (1993).
- [42] L. A. N. Amaral, A.-L. Barabási, and H. E. Stanley, Phys. Rev. Lett. **73**, 62 (1994); H. A. Makse, A.-L. Barabási, and H. E. Stanley (unpublished).
- [43] L.-H. Tang, M. Kardar, and D. Dhar, Phys. Rev. Lett. **74**, 920 (1995).
- [44] S. Havlin, L. A. N. Amaral, S. V. Buldyrev, S. T. Harrington, and H. E. Stanley, Phys. Rev. Lett. **74**, 4205 (1995).
- [45] S. V. Buldyrev, S. Havlin, J. Kertész, R. Sadr, and H. E. Stanley, Phys. Rev. E **52**, xxx (1 July 1995).
- [46] H. A. Makse, Ph. D. Thesis, Boston University (1996).
- [47] H. A. Makse and L. A. N. Amaral (unpublished).
- [48] G. Grinstein and S.-K. Ma, Phys. Rev. B **28**, 2588 (1983).
- [49] T. Nattermann, S. Stepanov, L.-H. Tang, and H. Leschhorn, J. Phys. II France **2**, 1483 (1992).

- [50] O. Narayan and D. S. Fisher, Phys. Rev. B **48**, 7030 (1993).
- [51] R. Bruinsma and G. Aeppli, Phys. Rev. Lett. **52**, 1547 (1984).
- [52] J. Krug and H. Spohn, Phys. Rev. Lett. **64**, 2332 (1990).
- [53] We introduce this time-dependent randomness in the model to mimic the experimental fact that for $F > F_c$, a transition to the KPZ behavior with annealed disorder is observed for $\ell \gg \xi$. In fact, Eqs. (3.1) and (3.3) should also include annealed disorder terms. However, this annealed disorder is much weaker than the quenched disorder. For this reason, for $\ell \ll \xi$ the presence of time dependent disorder is irrelevant. A different situation occurs for $\ell \gg \xi$. In this case the effect of quenched disorder is no longer relevant, and even a weak annealed disorder becomes important.
- [54] The consistency of the argument developed in the text can be verified by expanding (4.8) to first order, whereupon we recover (4.6).
- [55] The justification of this particular rule lies not only on the computational simplifications that it affords but also on the experimental finding that overhangs do not play an important role in the scaling properties of the interface for imbibition.
- [56] As was shown in Refs. [12,13,17,33], the DPD-1 and DPD-2 models belong to the same universality class, with exponents $\alpha \approx 0.63$ and $\theta \approx 0.64$ [42]. The deviation of the numerical values in the exponents for the DPD-2 model can be explained by the slow convergence of this model to the asymptotic scaling regime. The large error bars for all models arise from the fact that simulations were done for relatively small systems. Despite the differences in the values of the scaling exponents, based on the numerical results combined with the exact results of Refs. [12,13,17,33], we conclude that the models, DPD-1, DPD-2, and DPD-3, share the same set of scaling exponents, thus belonging to the same universality class.
- [57] H. A. Makse, Phys. Rev. E **52**, xxx (1995).
- [58] As was noted by Koiller *et al.* [28], different methods of defining time in the RFIM lead to different values of the exponents. Here we applied one of the methods suggested in [28], in which the unit time corresponds to flip all unstable interface spins. The value of the exponent given in [28] was obtained assuming that the time it takes a spin to flip depends on the energy gain, for the system, in the flipping.
- [59] This mapping to DP is valid only for one-dimensional interfaces, for higher dimensions the properties of these models are related to *directed surfaces*, of which DP is a particular case, for a discussion see [17].
- [60] Our results show that for the FA regime, the RFIM behaves in a similar fashion to the models in the DPD universality class, in that the coefficient of the nonlinear term diverges at the depinning transition. However, we stress that this regime has little physical motivation, being its existence due to lattice effects.
- [61] K. Sneppen, Phys. Rev. Lett. **69**, 3539 (1992); L.-H. Tang and H. Leschhorn, *Ibid.* **70**, 3832 (1993); K. Sneppen and M. H. Jensen, *Ibid.* **70**, 3833 (1993).
- [62] K. Sneppen and M. H. Jensen, Phys. Rev. Lett. **71**, 101 (1993).
- [63] H. Leschhorn and L.-H. Tang, Phys. Rev. E **49**, 1238 (1994).
- [64] Z. Olami, I. Procaccia, and R. Zeitak, Phys. Rev. E **49**, 1232 (1994).
- [65] S. Maslov and M. Paczuski, Phys. Rev. E **50**, R643 (1994).
- [66] S. Das Sarma, S. V. Ghaisas, and J. M. Kim, Phys. Rev. E **49**, 122 (1994).
- [67] Since we want to calculate the scaling exponents we only need to consider the leading order terms. Hence, although Eqs. (5.5) and (5.6) are only valid for $\ell \ll L$, we can, to leading order, compare the two expressions when $\ell = L$.
- [68] Reference [33] measured $\beta_M \approx 0.63$. However, the large intrinsic width [69] of their variant of the DPD model, leads the authors of Ref. [33] to add a constant to their data, which probably altered the scaling of W for $t \ll t_\times$.
- [69] J. Kertész and D. Wolf, J. Phys. A **21**, 747 (1988).
- [70] *Fractals and Disordered Systems*, edited by A. Bunde and S. Havlin, (Springer-Verlag, Heidelberg, 1991); D. Stauffer and A. Aharony, *Introduction to Percolation Theory*, 2nd ed. (Taylor & Francis, London, 1992).
- [71] S. Havlin and D. Ben-Avraham, Adv. Phys. **36**, 695 (1987).
- [72] J. W. Essam, K. De’Bell, J. Adler, and F. M. Bhatti, Phys. Rev. B **33**, 1982 (1986); J. W. Essam, A. J. Guttmann, and K. De’Bell, J. Phys. A **21**, 3815 (1988).
- [73] B. Sapoval, M. Rosso, and J. F. Gouyet, J. Physique – Lett. **46**, L149 (1985); M. Rosso, J. F. Gouyet, and B. Sapoval, Phys. Rev. Lett. **57**, 3195 (1986).
- [74] D. Wilkinson, Phys. Rev. A **30**, 520 (1984); *Ibid.* **34**, 1380 (1986).
- [75] A. Birovljev, L. Furuberg, J. Feder, T. Jøssang, K. J. Måløy, and A. Aharony, Phys. Rev. Lett. **67**, 584 (1991).
- [76] A. Hansen, T. Aukrust, J. M. Houlrik, and I. Webman, J. Phys. A: Math. Gen. **23**, L145 (1990); A. Hansen and J. M. Houlrik, J. Phys. A: Math. Gen. **24**, 2377 (1991).

FIG. 1. The depinning transition. In the “pinned phase,” $F < F_c$, the velocity of the interface is zero. In the “moving phase,” $F > F_c$, the interface moves with an average velocity $v \equiv v(F)$, where $v(F) \sim (F - F_c)^\theta$ for F close to F_c , and $v(f) \sim F$ for $F \gg F_c$. Thus, the velocity plays the role of the order parameter of the transition.

FIG. 2. Values of the roughness exponent α from most of the experiments, simulations and theoretical works reported in the literature. The experimental points are, reading from left to right, from Refs. [8], [9], [10] (a range of values is reported of which the extremes are plotted), [12-17], [11]. The simulation points are, reading from left to right, from Refs. [17] (a range of values is reported of which the extremes are plotted), [29], [12-17], [32], [31], [34], [33], [40], [27-28], [45], [46]. Finally, the theoretical points, again reading from left to right, are from Refs. [48] and [49]. Visually apparent is the wide spread of the results. To guide the eye, we indicate the values of α predicted by the KPZ equation with annealed disorder (bottom line), the DPD universality class in the pinned phase and moving phases (middle lines), and the QEW universality class (top line). We can see that most results for simulations and theoretical calculations are close to either the DPD or the QEW line. However, for the experimental results, the agreement is not so good. In the text we argue that the reasons for these disagreements are the crossover present in the moving phase for both universality classes, and the fact that for the DPD universality class $\alpha_M \neq \alpha_P$.

FIG. 3. *DPD-1 model*. (a) Dependence on the tilt m of the average velocity in $1 + 1$ dimensions. Data for different values of the force $f = (F - F_c)/F_c$ are indicated by different symbols, ranging from 0.016 (bottom curve) to 0.350 (top curve). The system size is $L = 512$ and each result was averaged over 30 realizations of the disorder. (b) Data collapse of the velocities according to (4.7) using the values for the DPD-3 model exponents (Table I).

FIG. 4. Here we exemplify the “noncrossing” effect on the velocity parabolas. We show a perfect parabolic behavior for two different forces, $f_1 > f_2$ (dashed lines) as predicted by Eq. (4.3). Also shown is the “curving back” of the velocity curve for the smaller force f_2 (solid line) which is necessary in order not to cross the velocity curve for f_1 .

FIG. 5. *DPD-2 model*. (a) Dependence on the tilt m of the average velocity in $1 + 1$ dimensions. Data for different forces f are indicated by different symbols, ranging from 0.0149 (bottom curve) to 0.0719 (top curve). The system size is 512 and each result was averaged over 30 realizations of the disorder. (b) Data collapse of the velocities according to (4.7) using the values for the DPD-2 model exponents (Table I).

FIG. 6. *DPD-3 model*. (a) Dependence on the tilt m of the average velocity in $1 + 1$ dimensions. Data for different values of the force f are indicated by different symbols, ranging from 0.0204 (bottom curve) to 0.2454 (top curve). The system size is $L = 1024$ and each result was averaged over 30 realizations of the disorder. (b) Data collapse of the velocities according to (4.7) using the values for the DPD-3 model exponents (Table I).

FIG. 7. *QEW-1 model*. Dependence on the tilt m of the average velocity in $1 + 1$ dimensions. Data for different values of the force f are indicated by different symbols, ranging from 0.0125 (bottom curve) to 0.075 (top curve). The system size is $L = 1024$ and each result was averaged over 30 realizations of the disorder. We can see clearly that $\lambda = 0$.

FIG. 8. *RFIM*. (a) Dependence on the tilt m of the average velocity in $2 + 1$ dimensions. Data for different values of the force f are indicated by different symbols, ranging from 0.014 (bottom curve) to 0.143 (top curve). The system size is $L^2 = 40 \times 40$, and $\Delta = 3$ (SA regime). (b) Data collapse of the velocities according to (4.7) using the values for the RFIM exponents (Table I).

FIG. 9. Schematic representation of the scaling behavior of the coefficient λ of the nonlinear term for the two universality classes. For the DPD universality class we see that λ diverges at the depinning transition, while for the QEW universality class it vanishes to zero at the transition.

FIG. 10. *DPD universality class*. (a) Plot of the local width w as a function of ℓ for a pinned and a moving interface. The different roughness exponent is clear. The system size is $L = 10480$ and each result was averaged over 50 realizations of the disorder. (b) Plot of the local width in the moving phase for several values of the driving force. (c) Data collapse of the widths according to (5.3). (d) Data collapse for $f = 0.0583$, and for systems of different size L . Visually apparent is the fact that the deviations from scaling observed in (c) are due to finite size effects.

FIG. 11. *DPD universality class*. (a) Plot of the global width W as a function of time the moving phase interface. The system size is $L = 10480$ and each result was averaged over 50 realizations of the disorder. (b) Data collapse of the widths according to (5.11).

FIG. 12. Anomalous scaling of the local width for the QEW universality class. (a) Interfaces generated with the QEW-2 model, at the depinning transition, for system of sizes $L = 128, 256, 512, 1024$. We note that the local slopes increase with the system size. (b) Plot of the scaling of the local width as a function of L , for two given values of ℓ . The fit corresponds to $\alpha_G - \alpha_P \approx 0.25$.

FIG. 13. *QEW universality class*. (a) Plot of the local width in the moving phase for several values of the reduced force. The system size is $L = 5524$ and each result was averaged over 100 realizations of the disorder. (b) Data collapse of the widths according to (5.3).

FIG. 14. *QEW universality class*. (a) Plot of the global width W as a function of time for the moving phase. The system size is $L = 5524$ and each result was averaged over 100 realizations of the disorder. (b) Data collapse of the widths according to (5.11).

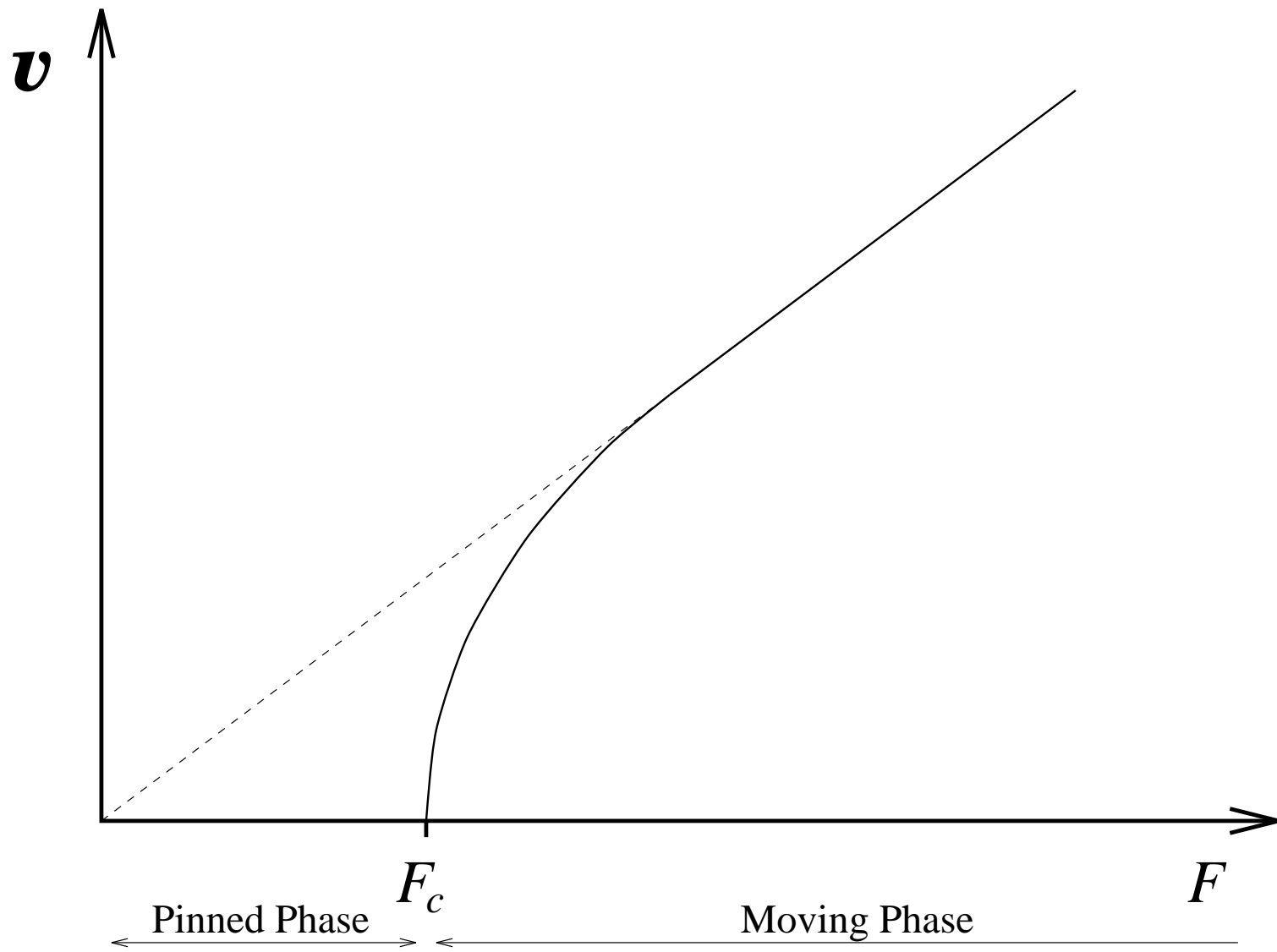
TABLE I. Exponents for the six models studied (see definitions in the text). A negative value of ϕ means that $\lambda \rightarrow 0$ when $f \rightarrow 0$ [cf. Eq. (4.5)]. We argue in the text that the models above the horizontal line (DPD-1, DPD-2, and DPD-3) belong to the universality class of Eq. (3.3) and can be mapped, in $1 + 1$ dimensions, to DP. The models below the line belong to the universality class of Eq. (3.1). See [56] for a discussion on the values of the exponents for the DPD-2 model.

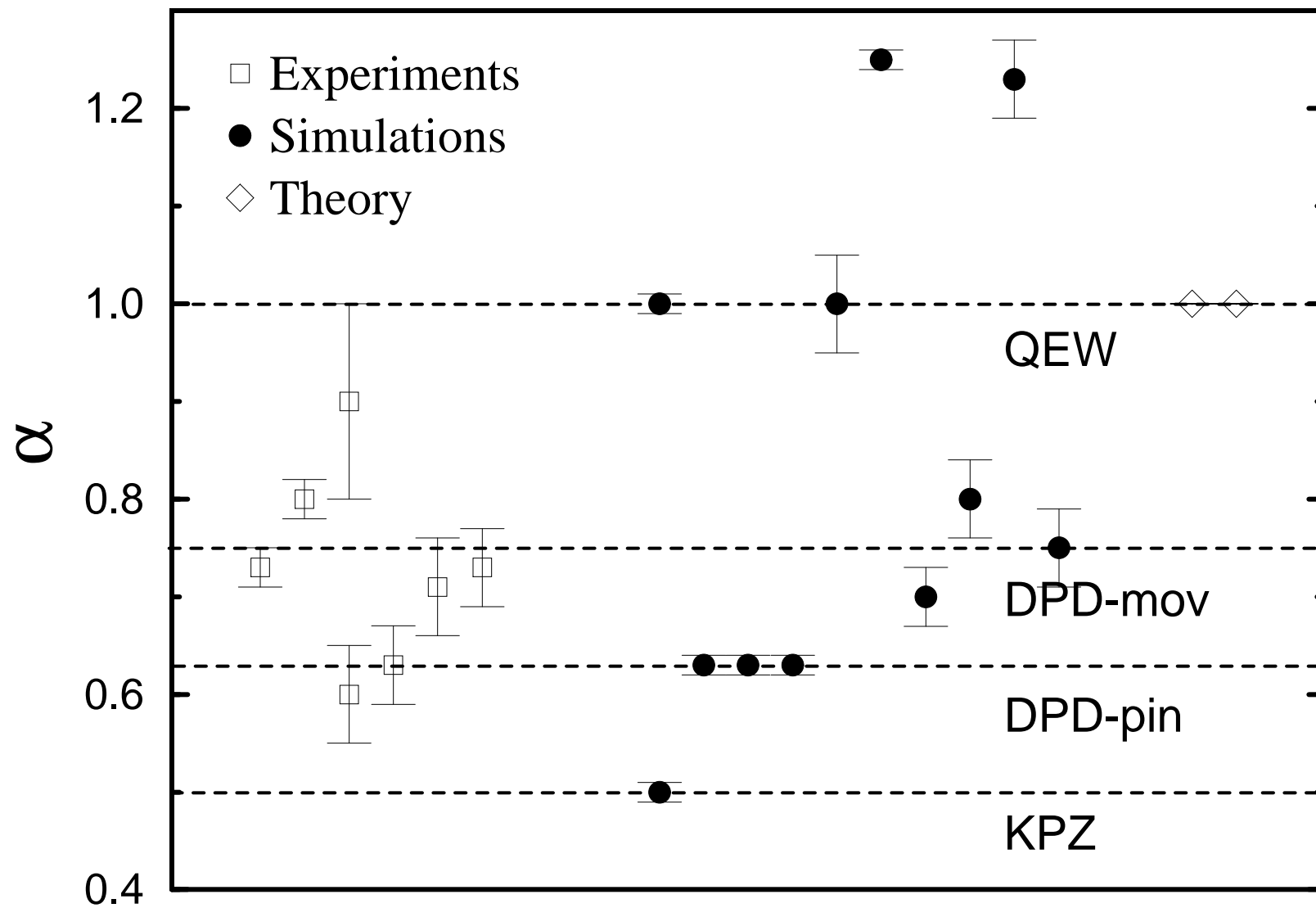
Model	1 + 1 dimensions		2 + 1 dimensions	
	θ	ϕ	θ	ϕ
DPD-1	0.64 ± 0.08	0.64 ± 0.08	0.80 ± 0.12	0.30 ± 0.12
DPD-2	0.59 ± 0.12	0.55 ± 0.12		
DPD-3	0.70 ± 0.12	0.65 ± 0.12		
QEW-1	0.26 ± 0.07	—		
QEW-2	0.24 ± 0.03	—		
FA	0.9 ± 0.2	1.8 ± 0.2		
RFIM SA	—	—	0.60 ± 0.11	-0.70 ± 0.11
SS	0.31 ± 0.08	-0.65 ± 0.13		

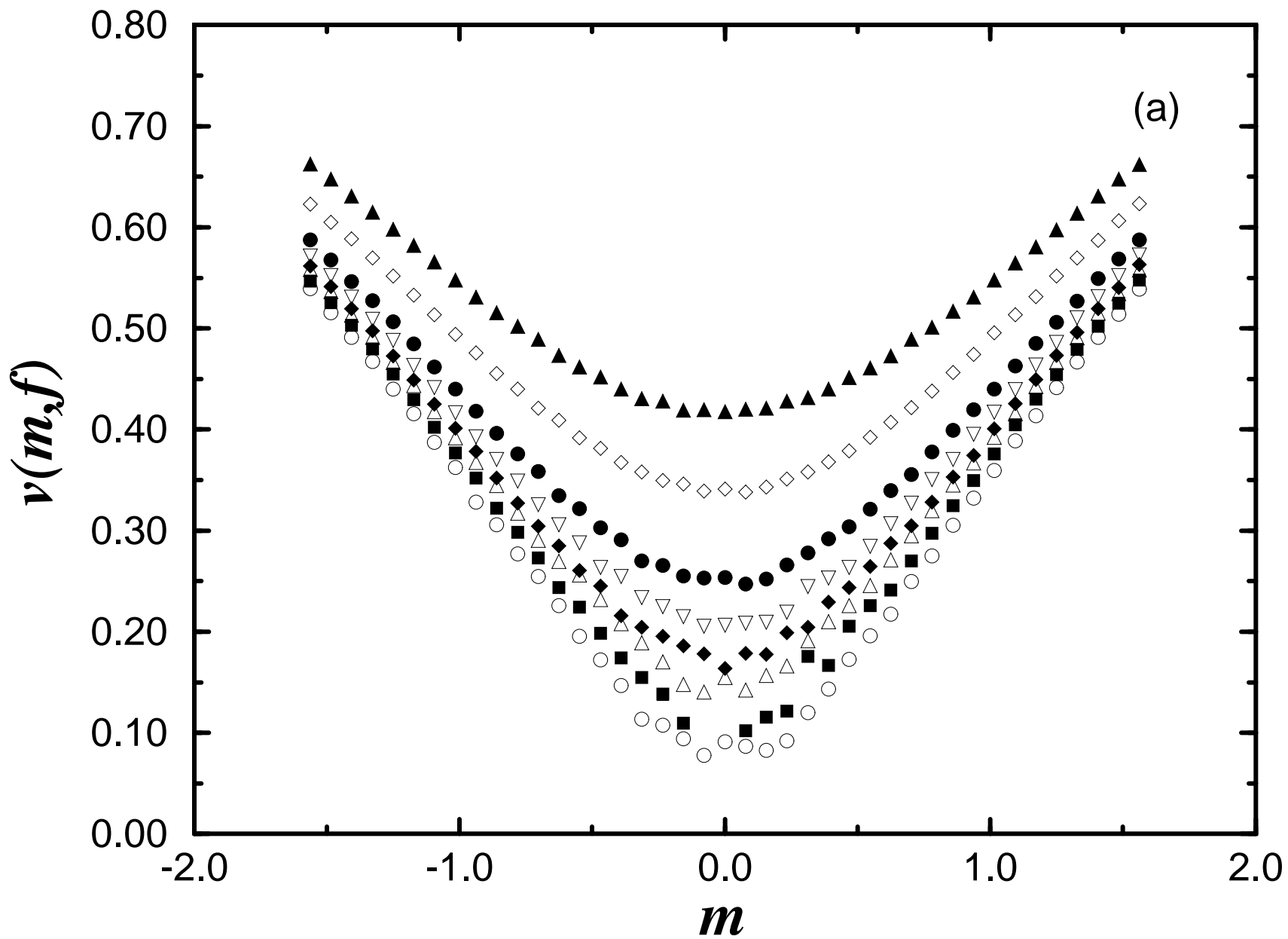
TABLE II. Critical exponents for the two universality classes studied in this paper. The subscript “ P ” refers to the *pinned* phase, the subscript “ M ” denotes the quenched disorder regime in the *moving* phase, and the subscript “ A ” refers to the *annealed disorder* regime. The exponents z and z_A were calculated from scaling relations, while the remaining exponents were calculated directly in the simulations.

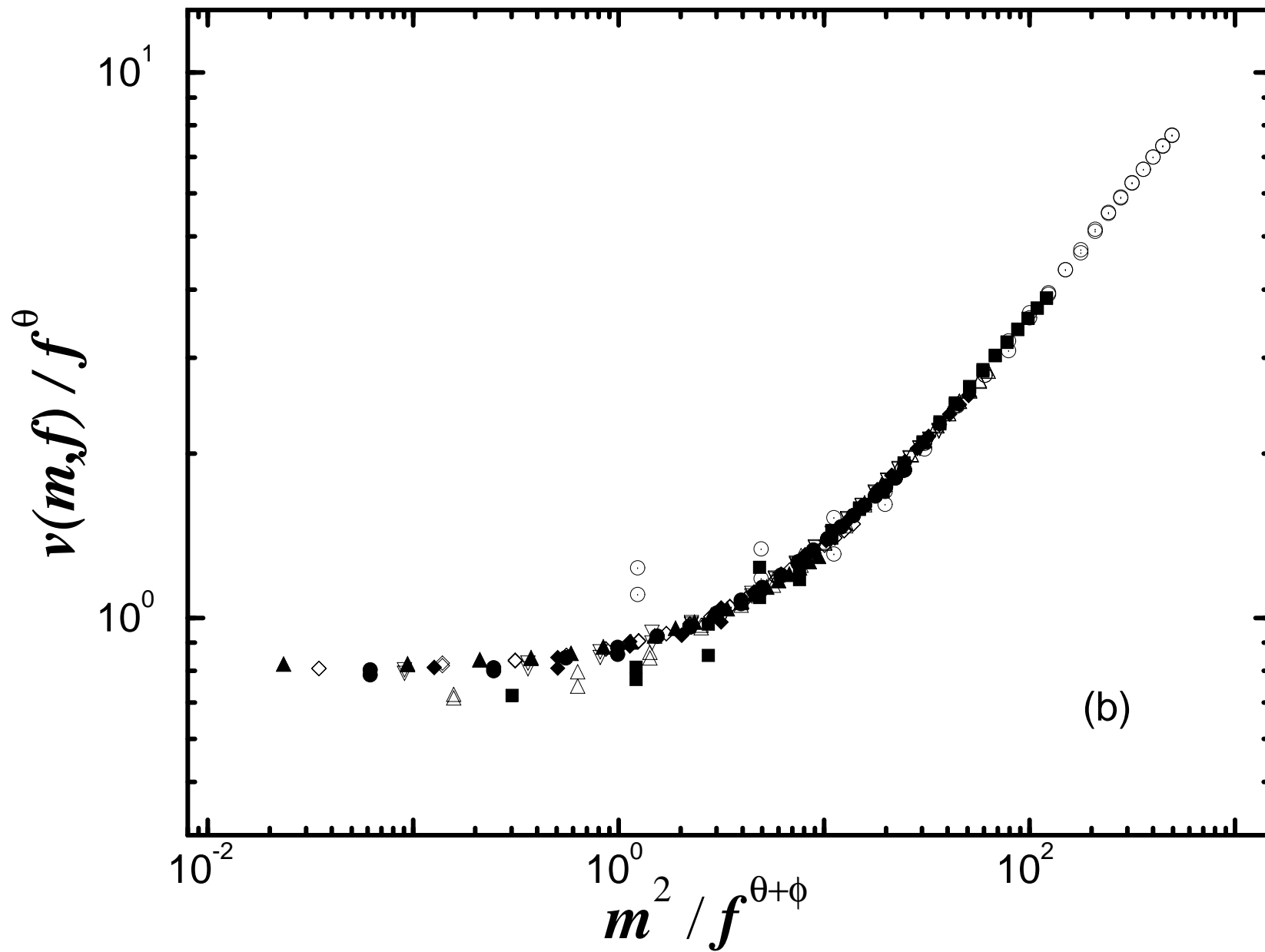
Exponents	DPD	QEW
α_P	0.63 ± 0.03	0.92 ± 0.04
α_M	0.75 ± 0.04	0.92 ± 0.04
α_A	0.50 ± 0.04	0.46 ± 0.04
α_G	—	1.23 ± 0.04
β_P	0.67 ± 0.05	0.85 ± 0.03
β_M	0.74 ± 0.06	0.86 ± 0.03
β_A	0.30 ± 0.04	0.25 ± 0.04
z	1.01 ± 0.10	1.45 ± 0.07
z_A	1.67 ± 0.26	2.09 ± 0.40
ν	1.73 ± 0.04	1.35 ± 0.04
θ	0.64 ± 0.12	0.24 ± 0.03
φ_M	-0.12 ± 0.06	0.44 ± 0.05
φ_A	0.34 ± 0.06	0.99 ± 0.05
κ_M	-0.11 ± 0.06	0.00 ± 0.06
κ_A	0.65 ± 0.06	1.15 ± 0.06

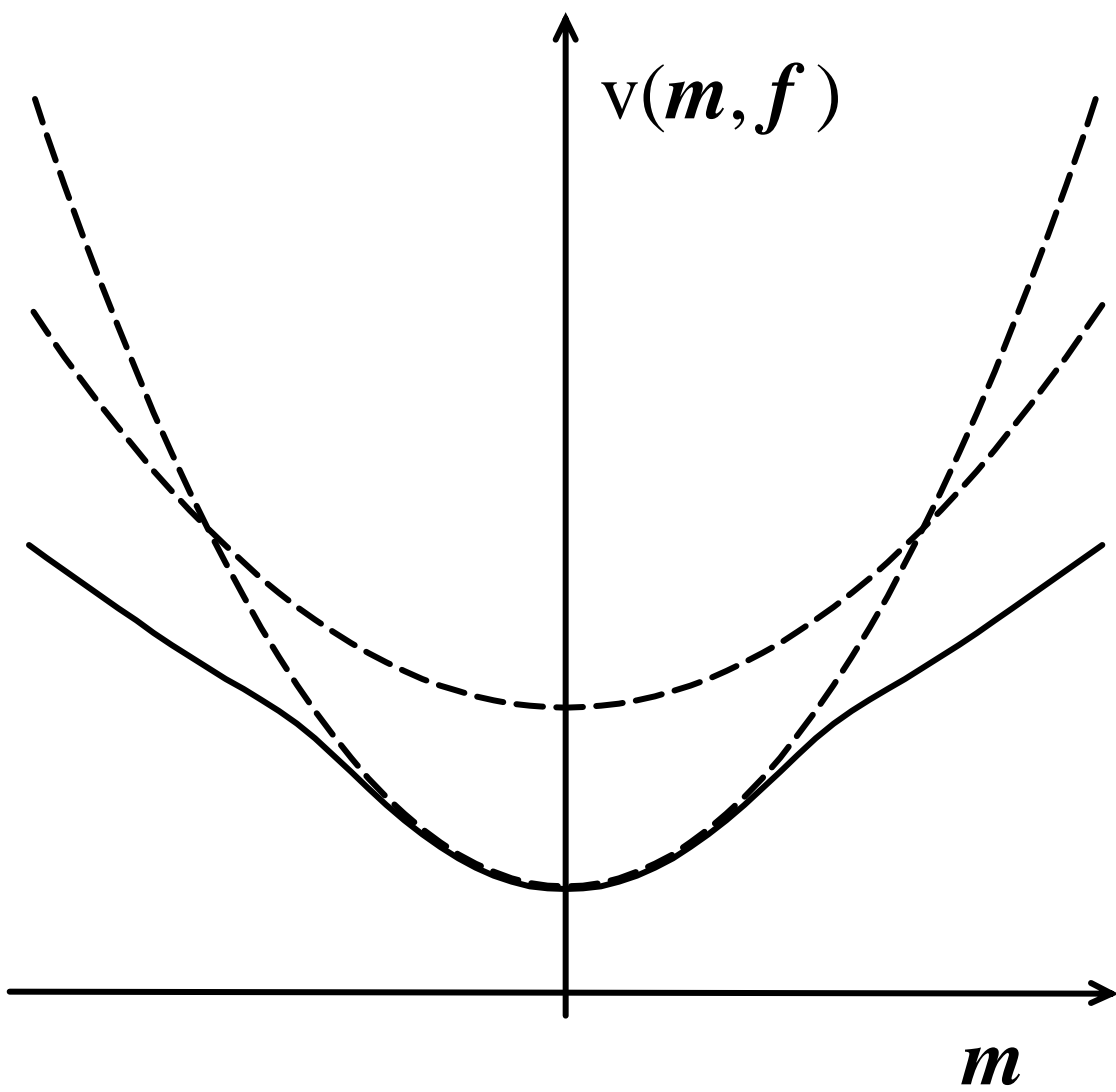
FIG. 15. Simulation results for the width $w(\ell, g)$ of the pinned interface in $1 + 1$ dimensions, where g is the gradient in ρ . (a) The widths for values of the gradient ranging from $1/70$ to $1/7680$. The system size is 10480 and each result is averaged over 30 realizations of the disorder. (b) Data collapse of these results according to the scaling form (B4), using the values of the exponents given in (B5).

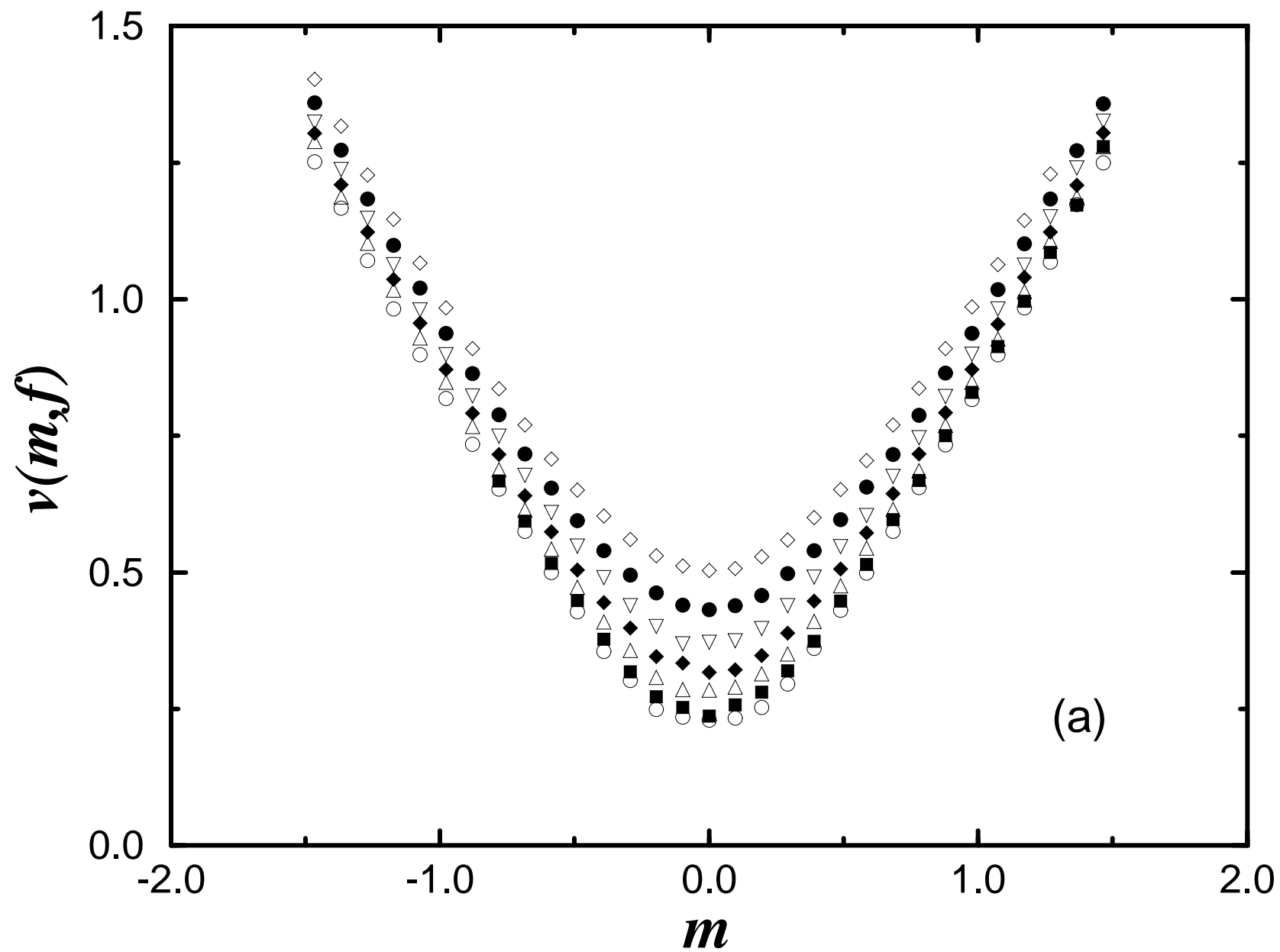


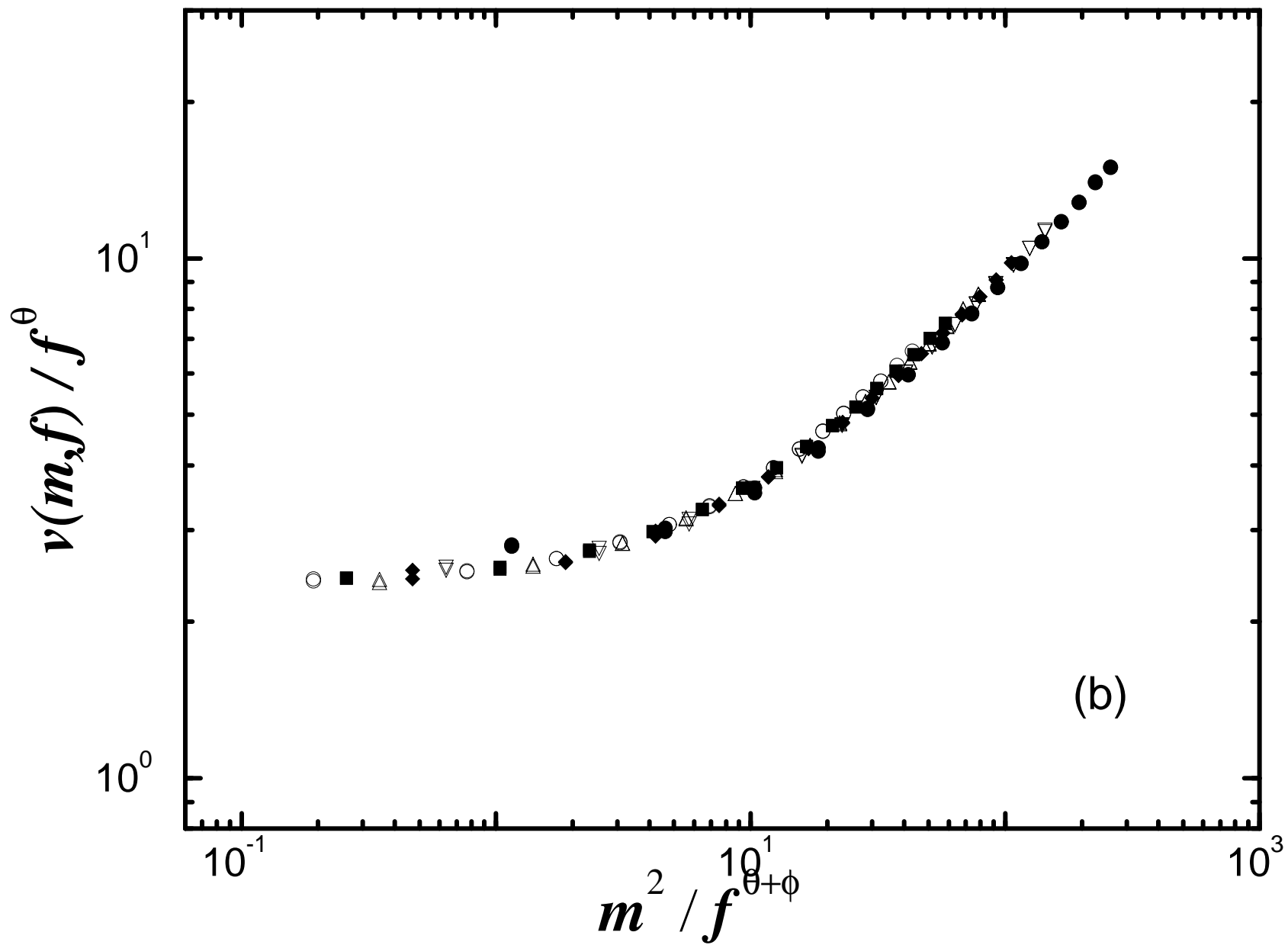


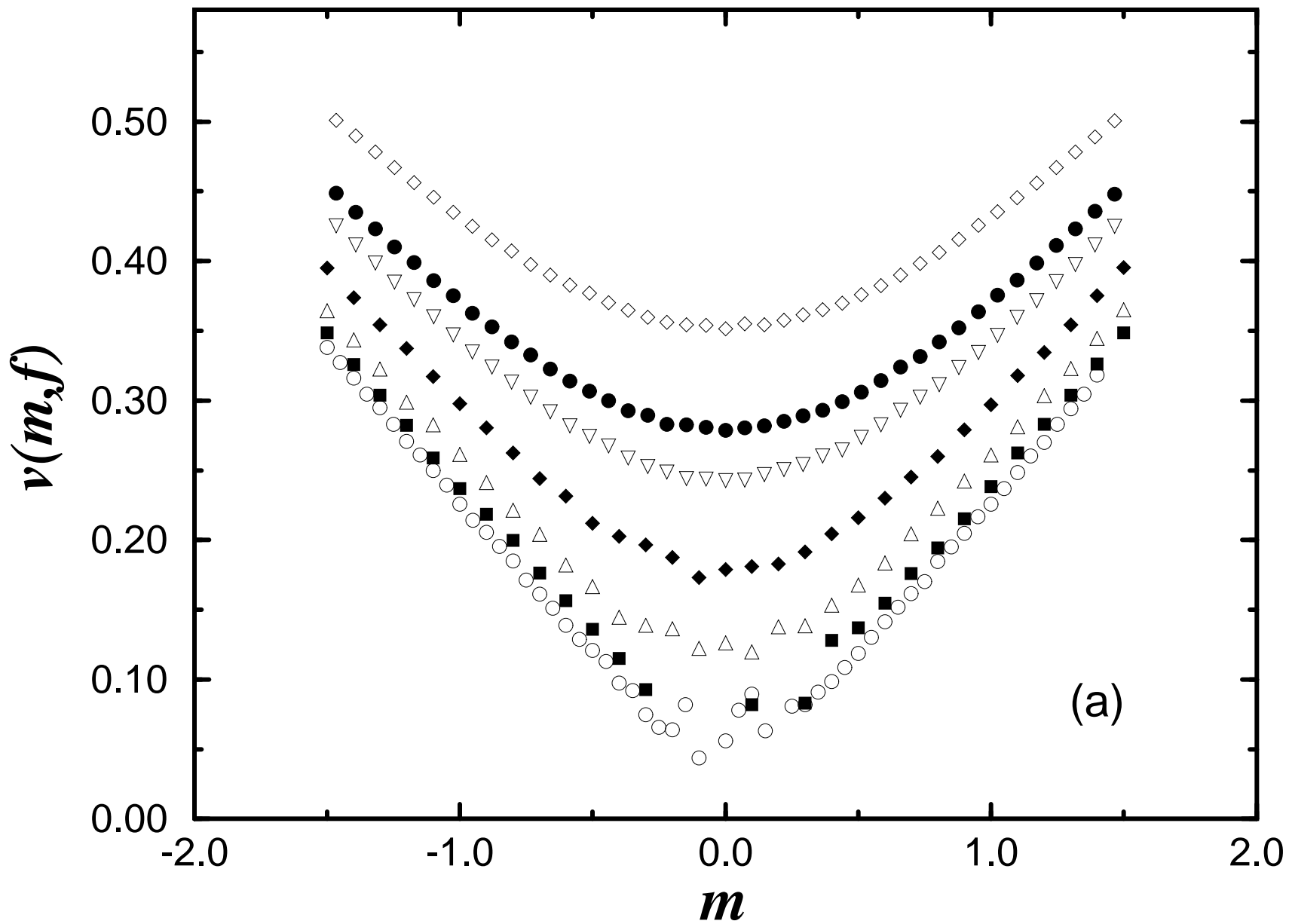


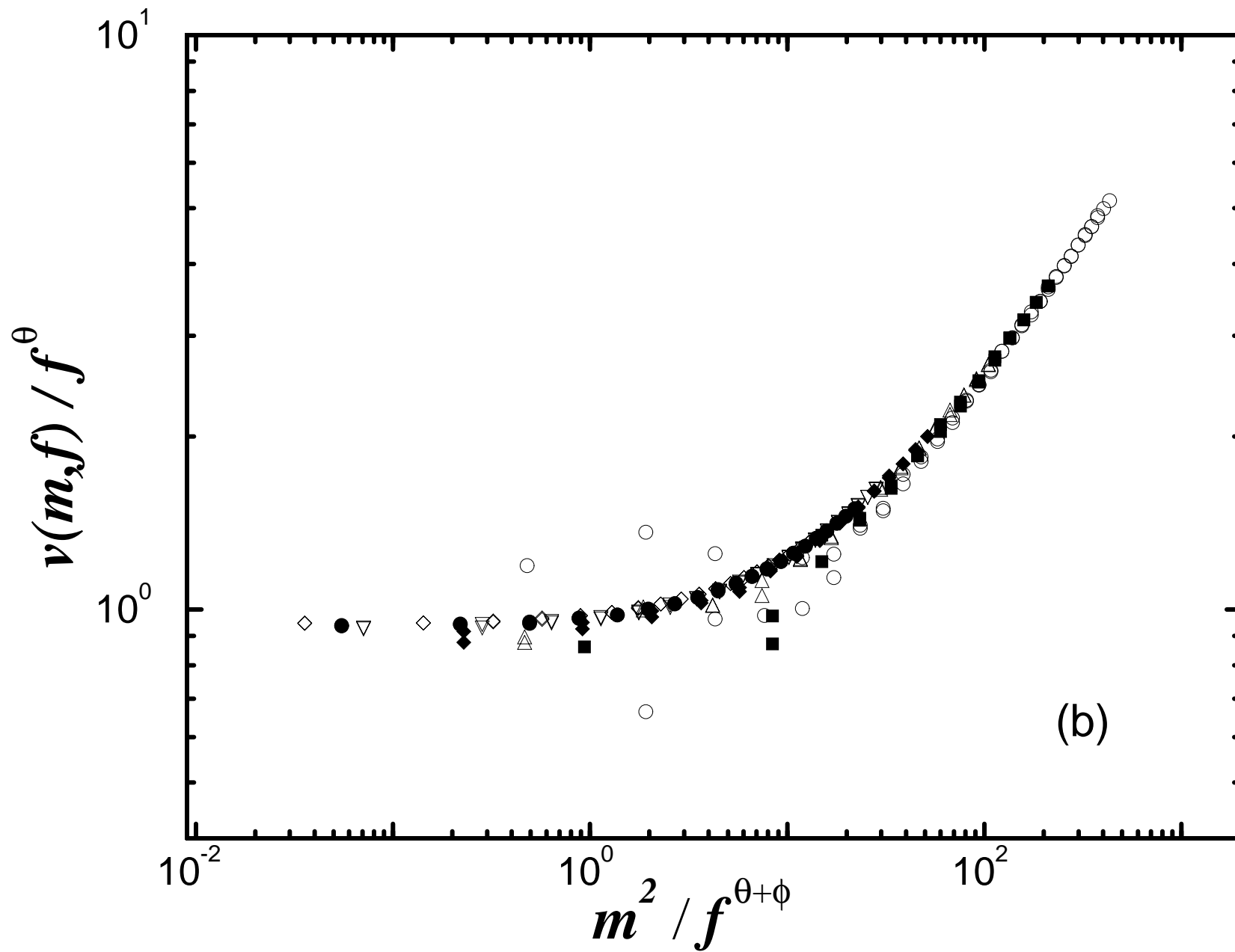


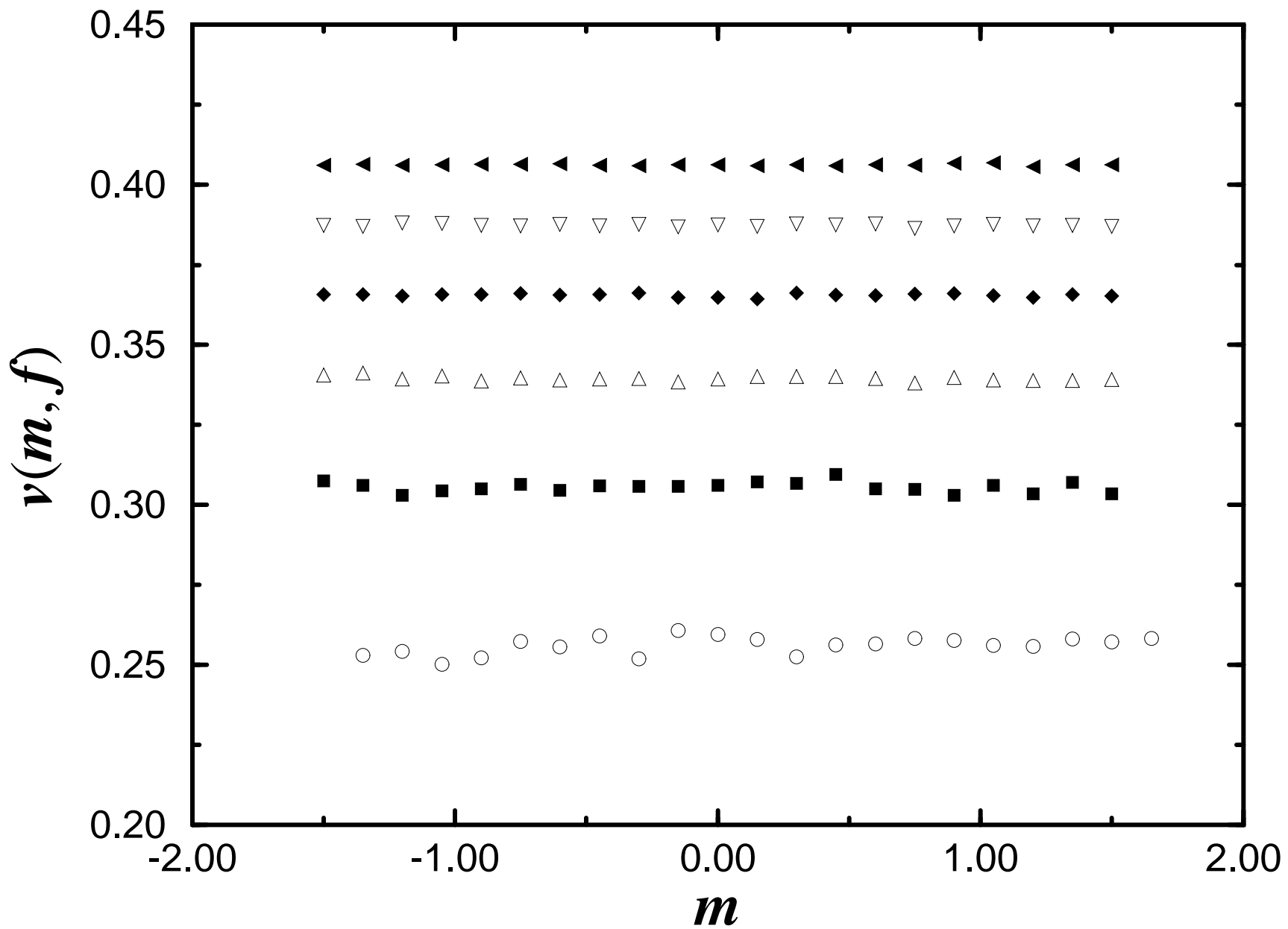


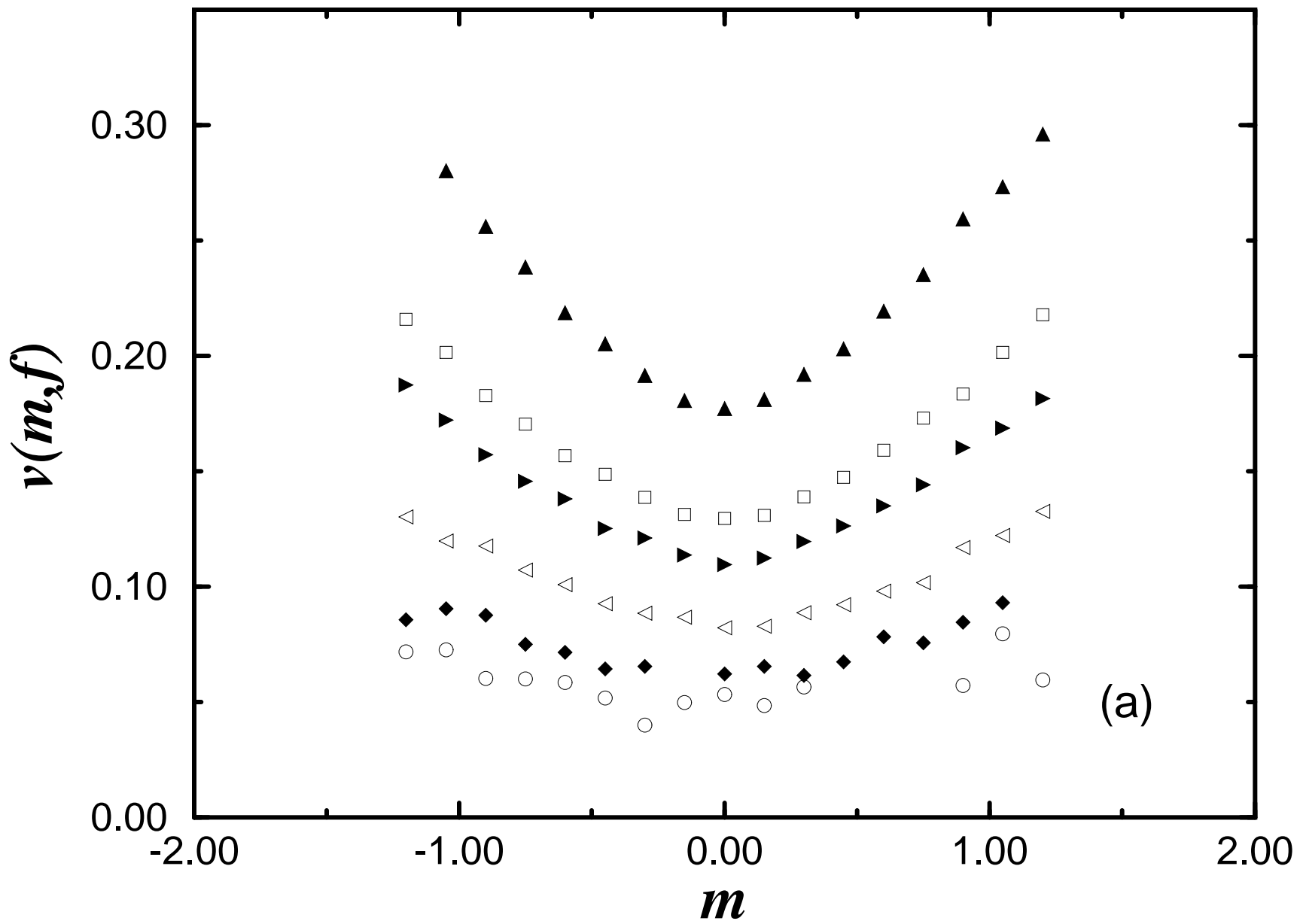












(a)

